ELSEVIER

Quaternary Science Reviews ▮ (▮▮▮▮) ▮▮▮–▮▮▮

QSR

Great-earthquake paleogeodesy and tsunamis of the past 2000 years at Alsea Bay, central Oregon coast, USA

Alan R. Nelson[a,*], Yuki Sawai[b], Anne E. Jennings[c], Lee-Ann Bradley[a], Linda Gerson[c], Brian L. Sherrod[d], Jennifer Sabean[e], Benjamin P. Horton[f]

[a]*Geologic Hazards Team, US Geological Survey, MS 966, P.O. Box 25046, Denver, CO 80225, USA*
[b]*Active Fault Research Center, Institute of Advanced Industrial Science and Technology, Tsukuba, Japan*
[c]*Institute of Arctic and Alpine Research, University of Colorado, Boulder, CO 80309-0450, USA*
[d]*US Geological Survey, Department of Earth and Space Sciences, University of Washington, Seattle, WA 98195, USA*
[e]*Department of Earth Sciences, Simon Fraser University, 8888 University Dr., Burnaby, BC, Canada V5A 1S6*
[f]*Department of Earth & Environmental Science, University of Pennsylvania, 240 South 33rd Street, Philadelphia, PA 19104-6316, USA*

Received 12 September 2007; received in revised form 21 December 2007; accepted 2 January 2008

Abstract

The width of plate-boundary fault rupture at the Cascadia subduction zone, a dimension related to earthquake magnitude, remains uncertain because of the lack of quantitative information about land-level movements during past great-earthquake deformation cycles. Beneath a marsh at Alsea Bay, on the central Oregon coast, four sheets of tsunami-deposited sand blanket contacts between tidal mud and peat. Radiocarbon ages for the sheets match ages for similar evidence of regional coseismic subsidence and tsunamis during four of Cascadia's great earthquakes. Barring rapid, unrecorded postseismic uplift, reconstruction of changes in land level from core samples using diatom and foraminiferal transfer functions includes modest coseismic subsidence (0.4 ± 0.2 m) during the four earthquakes. Interpretation is complicated, however, by the 30–38% of potentially unreliable transfer function values from samples with poor analogs in modern diatom and foraminiferal assemblages. Reconstructions of coseismic subsidence using good-analog samples range from 0.46 ± 0.12 to 0.09 ± 0.20 m showing greater variability than implied by sample-specific errors. From apparent high rates of land uplift following subsidence and tsunamis, we infer that postseismic rebound caused by slip on deep parts of the plate boundary and (or) viscoelastic stress relaxation in the upper plate may be almost as large as coseismic subsidence. Modest coseismic subsidence 100 km landward of the deformation front implies that plate-boundary ruptures in central Oregon were largely offshore. Ruptures may have been long and narrow during earthquakes near magnitude 9, as suggested for the AD 1700 earthquake, or of smaller and more variable dimensions and magnitudes.

1. Introduction

Despite consensus that the history of the Cascadia subduction zone includes plate-boundary earthquakes of magnitude 9 (M9; Clague et al., 2000a; Goldfinger et al., 2003; Satake et al., 2003; Kelsey et al., 2005; Satake and Atwater, 2007; Fig. 1), Cascadia's earthquake hazard is uncertain. For example, in southern Cascadia great earthquakes in the lower magnitude 8 range may be more frequent than earthquakes near M9—or evidence of M8 earthquakes and accompanying tsunamis may simply be better preserved than in northern Cascadia (Nelson et al., 2006). Paleoseismology of the past two decades sought to infer past earthquake magnitudes through estimates of rupture length (e.g., Atwater et al., 1991; Nelson et al., 1995), but rupture width is an equally critical aspect of geophysical models of the next great Cascadia earthquake. Forecasts of earthquake ground motions that will strike cities of central western North America are calculated from the closest approach of earthquake rupture zones (Frankel et al., 2002). Although modeling of plate-boundary rupture zones has improved dramatically over the past two decades (Hyndman and Wang, 1995; Wang et al., 2003), the inland

*Corresponding author. Tel.: +1 303 273 8592; fax: +1 303 273 8600.
E-mail address: anelson@usgs.gov (A.R. Nelson).

0277-3791/$ - see front matter © 2008 Elsevier Ltd. All rights reserved.
doi:10.1016/j.quascirev.2008.01.001

Please cite this article as: Nelson, A.R., et al., Great-earthquake paleogeodesy and tsunamis of the past 2000 years at Alsea Bay, central Oregon coast, USA. Quaternary Science Reviews (2008), doi:10.1016/j.quascirev.2008.01.001

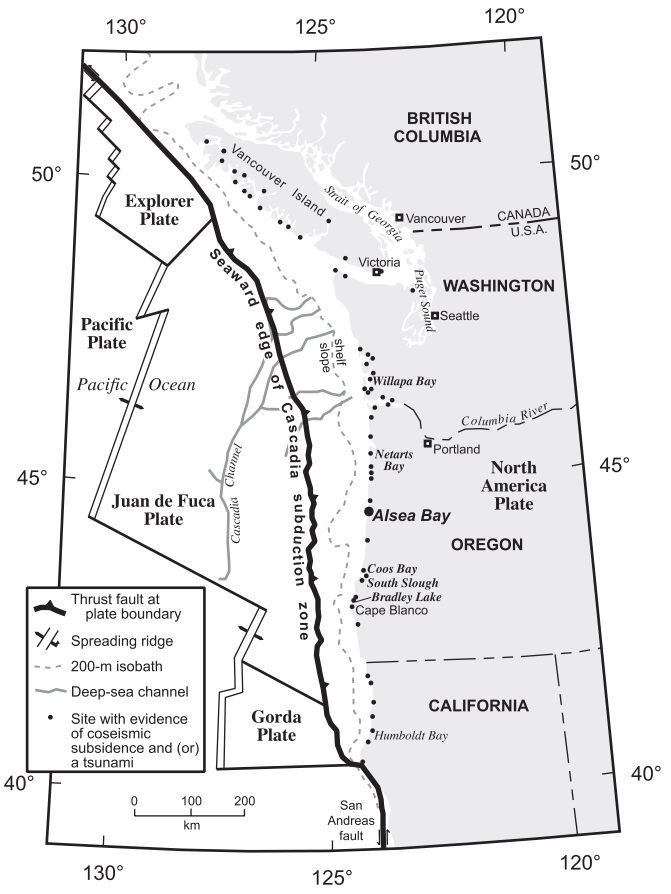

Fig. 1. Major features of the Cascadia subduction zone (modified from Atwater and Hemphill-Haley, 1997; Clague, 1997) showing the location of Alsea Bay on the central Oregon coast. The trace of the Cascadia thrust fault (barbed line) is placed at the bathymetric boundary between the continental slope and abyssal plain. Dots mark sites with evidence of subsidence and (or) tsunamis accompanying Cascadia subduction-zone earthquakes (Atwater et al., 1995, 2005; Clague et al., 2000b; Satake et al., 2003; Williams et al., 2005).

extent of ruptures during earthquakes of differing magnitude remains uncertain, partly because of the lack of quantitative information about land-level movements during past earthquake deformation cycles. Modelers agree that ruptures extending well beneath the coast would cause substantial sudden subsidence along much of the Cascadia coast, whereas little subsidence would accompany offshore ruptures (Wells et al., 2003; Leonard et al., 2004).

Mapping the width of past great-earthquake ruptures at Cascadia requires quantitative estimates of coseismic coastal subsidence. Previous estimates of subsidence for most Oregon coastal sites, collected during reconnaissance studies in the late 1980s and early 1990s, are based largely on qualitative or semi-quantitative field data (e.g., Leonard et al., 2004), some of which are probably unrelated to land-level movement during earthquake cycles (Long and Shennan, 1998; Nelson et al., 1998). Abrupt lithologic changes in wetland cores and outcrops may reflect either sudden subsidence during great earthquakes, with or without deposition of sandy sediment by tsunamis, or local hydrographic changes in estuaries induced by large storms, floods, or slow sea-level rise (Nelson et al., 1996a; Witter et al., 2001). Microfossils—such as pollen, diatoms, or foraminifera—in tidal sediment are studied as quantitative archives of relative sea-level change that help distinguish seismic from nonseismic sea-level changes (Shennan et al., 1998; Denys and de Wolf, 1999; e.g., Hughes et al., 2002a; Sawai et al., 2004a; Shennan and Hamilton, 2006). Such biostratigraphic methods have been applied at less than a quarter of the more than 35 Cascadia estuaries; statistically supported studies with errors on past subsidence events of <0.5 m are limited to five estuaries.

In the late 1990s, application of transfer function analysis—widely used on microfossils from deep marine cores to reconstruct climate change—revitalized studies of Holocene sea-level change, particularly in northwest Europe and eastern North America (e.g., Zong and Horton, 1999; Gehrels, 2000; Horton and Edwards, 2006). As first demonstrated at Cascadia with foraminiferal data from marshes of Vancouver Island (Guilbault et al., 1995, 1996), this statistical approach at least doubles the precision of estimates of sudden coseismic subsidence. With sufficient sample density, it also provides a continuous record of relative sea-level change during interseismic parts of the earthquake cycle—essential information for understanding the mechanics of plate-boundary ruptures in subduction zones (Long and Shennan, 1994; Atwater et al., 2004b; Natawidjaja et al., 2004; Sawai et al., 2004b; Hamilton et al., 2005; Shennan and Hamilton, 2006). Only in the past few years have such transfer functions been applied to earthquake and tsunami history on Cascadia's US coasts (Sabean, 2004).

In this paper, we map and date tidal lithofacies interrupted by sand sheets deposited by the tsunamis of Cascadia's four most recent great earthquakes on the eastern shore of Alsea Bay, at coastal Oregon's center (Fig. 1). The Alsea Bay site fills a gap—extending 25 km north and 52 km south—in estuarine archives of Cascadia earthquake history (Darienzo and Peterson, 1995). We apply transfer function analysis using diatoms and foraminifera from a tidal marsh core at the site to reconstruct elevation changes, especially amounts of coseismic subsidence during the earthquakes. Subsidence estimates of 0.4 ± 0.2 m combined with earlier geophysical modeling of plate-boundary deformation imply that during the past 2000 years the plate-boundary in central Oregon has largely ruptured offshore.

Tidal marshes, whose sediment preserves stratigraphic evidence of regional coseismic subsidence and tsunamis, line the northeastern and southeastern shores of Alsea Bay and extend 8 km up the Alsea River (Fig. 2A; Peterson and Darienzo, 1996; Priest and Allan, 2003). Although former shallow tidal channels were widened and deepened in the early twentieth century, the marshes we studied north of the deepened channels (Fig. 2B) are mostly undiked and little disturbed. The marshes face plentiful sources for

Please cite this article as: Nelson, A.R., et al., Great-earthquake paleogeodesy and tsunamis of the past 2000 years at Alsea Bay, central Oregon coast, USA. Quaternary Science Reviews (2008), doi:10.1016/j.quascirev.2008.01.001

tsunami-deposited sand: the low, 2-km-long sand spit that separates the west shore of the bay from the sea, and sand-floored channels hundreds of meters wide in the central part of the bay (Fig. 2A).

2. Lithostratigraphy

Tidal sediment beneath the marshes of eastern Alsea Bay (Figs. 2–5) records great plate-boundary earthquakes and accompanying tsunamis (Darienzo et al., 1994; Peterson and Darienzo, 1996). The sharp ($\leqslant$10 mm) to abrupt ($\leqslant$1 mm) contacts between muddy or sandy tide-flat sediment and underlying peaty sediment of former marshes (termed "peat–mud contacts", Nelson et al., 1996a; or "peat–sand contacts", Nelson et al., 2004; Figs. 4 and 5) are the most widely used criterion to infer sudden, coseismic sea-level changes caused by flexure of the upper plate of the subduction zone during plate-boundary earthquakes (Nelson et al., 1996a; e.g., Peterson et al., 2000; Witter et al., 2003). Variations in the sharpness of contacts, their lateral extent, and the range of contact-bounding lithologies, however, suggest that some sharp and most gradual contacts reflect local nonseismic changes in rates of sedimentation, erosion, marsh development, and relative sea-level rise (e.g., Nelson et al., 1996b, 2004; Shennan et al., 1998; Allen, 2000). We examined lithostratigraphy in 25-mm-diameter cores throughout the marshes to evaluate four of the five criteria of Nelson et al. (1996a) for inferring coseismic subsidence from marsh stratigraphic sequences: the suddenness of submergence; the amount of submergence; the lateral extent of submerged tidal-wetland soils; and the coincidence of submergence with tsunami deposits. The fifth criteria, the degree of synchronicity of submergence events, is discussed more fully by Nelson et al. (2006).

2.1. Marsh cores

Of the 44 gouge cores and two vibrocores that we examined in the marshes of eastern Alsea Bay (Fig. 2), 23 were described in detail (9–19 (1σ range) stratigraphic units per meter of core) using the widely used Troels-Smith system (Troels-Smith, 1955; Long et al., 1999) for describing organic-rich sediments. Ten of the 23 cores

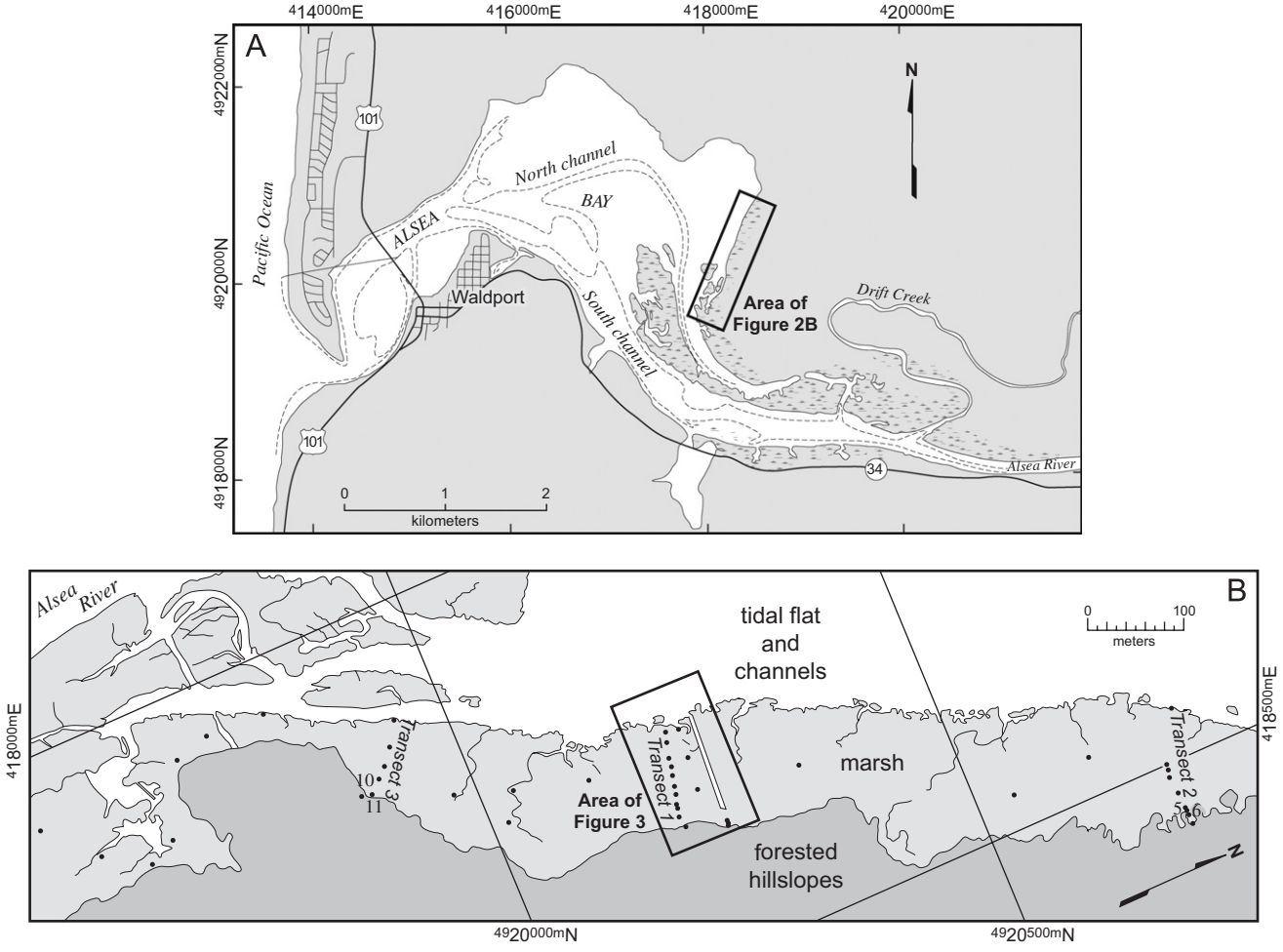

Fig. 2. (A) Map of Alsea Bay showing developed areas, major channels of the Alsea River (dashed lines), marshes in the eastern part of the bay (pattern), and area of Fig. 2B; (B) map of the eastern shore of Alsea Bay showing area of Fig. 3 and locations of 46 cores (dots), including cores 5 and 6 on transect 2, and cores 10 and 11 on transect 3 (Figs. 3–5).

Please cite this article as: Nelson, A.R., et al., Great-earthquake paleogeodesy and tsunamis of the past 2000 years at Alsea Bay, central Oregon coast, USA. Quaternary Science Reviews (2008), doi:10.1016/j.quascirev.2008.01.001

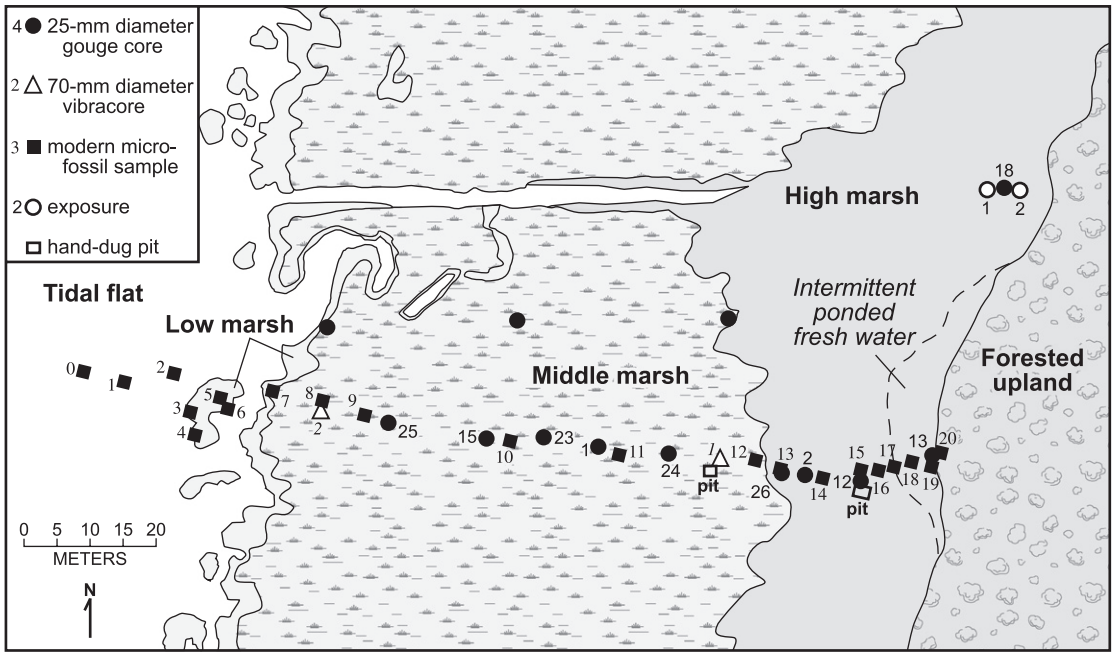

Fig. 3. Locations of gouge cores, vibrocores, modern samples of diatoms and foraminifers (Fig. 8; Tables SD1 and SD2), and exposures along and near transect 1 (Fig. 2B). The locations of a 0.5 × 0.5-m pit, 0.5 m deep, 2 m southwest of core V1 and a 1.5 × 2-m pit, 1.5 m deep, 1 m south of core 12 are also shown. Core 13 and modern samples 17–19 were collected on the east edge of the high marsh where freshwater is intermittently ponded against the forested hillslope. Exposures 1 and 2 are along a drainage ditch.

were photographed. Nineteen other cores were described in less detail, noting mostly major lithologies, macrofossils, and characteristics of sandy units and their contacts. Only 9 of the 44 cores reached depths of 4–5 m. Peterson and Darienzo (1996) described three 2.5–4.5-m long cores from the same marsh, spaced 270–620 m apart (area of Fig. 2B). Twenty 1–1.5-m-high outcrops along the North Channel and its inlets were also described or photographed for comparison with the 62 channel outcrops and 13 other cores studied by Peterson and Darienzo (1996, their Figs. 46 and 47) in Alsea River marshes to the south and southeast. Most of our core sites, outcrops, and benchmarks were located to within 3 m on enlargements of true-color air photographs (1:13,000 scale). We used a laser ranger to measure distances among core sites (error ±0.5 m; Fig. 2).

Mean tide level (MTL) at transect 1 was estimated by measuring the elevations of low tides (on 3 days) and high tides (on 2 days) relative to a temporary transect benchmark. We then compared the measurements with the predicted tide level at Waldport (National Ocean Service, 1987), 2.6 km to the west (Fig. 2), and interpolated between the temporary tide gauge measurements of Goodwin et al. (1970, their Fig. 7, 25 days of tidal records at Waldport and at a site 6 km east of our study site) to correct our estimates of MTL (+44 mm), MHHW (+12 mm), and MLLW (+98 mm) relative to the Waldport tide gauge. The elevations of transects 2 and 3 relative to MTL at transect 1 were estimated by simultaneously measuring the elevation of high tide on each transect (error <30 mm). Elevations of core sites along transects (Figs. 3–5) were measured using an automatic level (transect 1; error ±8 mm) or rotating laser level (transects 2 and 3; error <20 mm).

2.2. Sand sheets

Four sheets of sand (labeled A–D, Figs. 4 and 5) in the upper 2 m of tidal sediment beneath the marshes of eastern Alsea Bay have characteristics typical of tsunami deposits in other Cascadia marshes (Peterson and Darienzo, 1996; e.g., Benson et al., 1997; Clague et al., 2000b; Witter et al., 2003; Nelson et al., 2004; Williams et al., 2005; Schlichting and Peterson, 2006) and so help confirm that the contacts blanketed by the sheets coincide with great earthquakes. Sand sheets A and B are found in 36 of 44 cores, whereas sheets C and D were identified in 29 cores. The four sheets appear in a core described by Peterson and Darienzo (1996) about 150–300 m south of transect 2 (Fig. 2B). All four sheets can be correlated over the 850 m between transects 2 and 3 (Figs. 2B and 5); sheets A and B have been mapped from transect 2 eastward along the South Channel, a distance of more than 2 km (Fig. 2A; Peterson and Darienzo, 1996). Sheet thicknesses are highly variable in cores (Table 1, Figs. 4 and 5), exposures near the upper edge of the marsh, and outcrops along Alsea River channels. Lower sandy beds of sheets consist of clean to slightly muddy, fine-to-very-fine sand (measurements by Peterson and Darienzo (1996) show 58–88% sand in some of these beds). The beds grade upward into slightly muddy to muddy, very-fine to extremely fine, sand and coarse silt.

Please cite this article as: Nelson, A.R., et al., Great-earthquake paleogeodesy and tsunamis of the past 2000 years at Alsea Bay, central Oregon coast, USA. Quaternary Science Reviews (2008), doi:10.1016/j.quascirev.2008.01.001

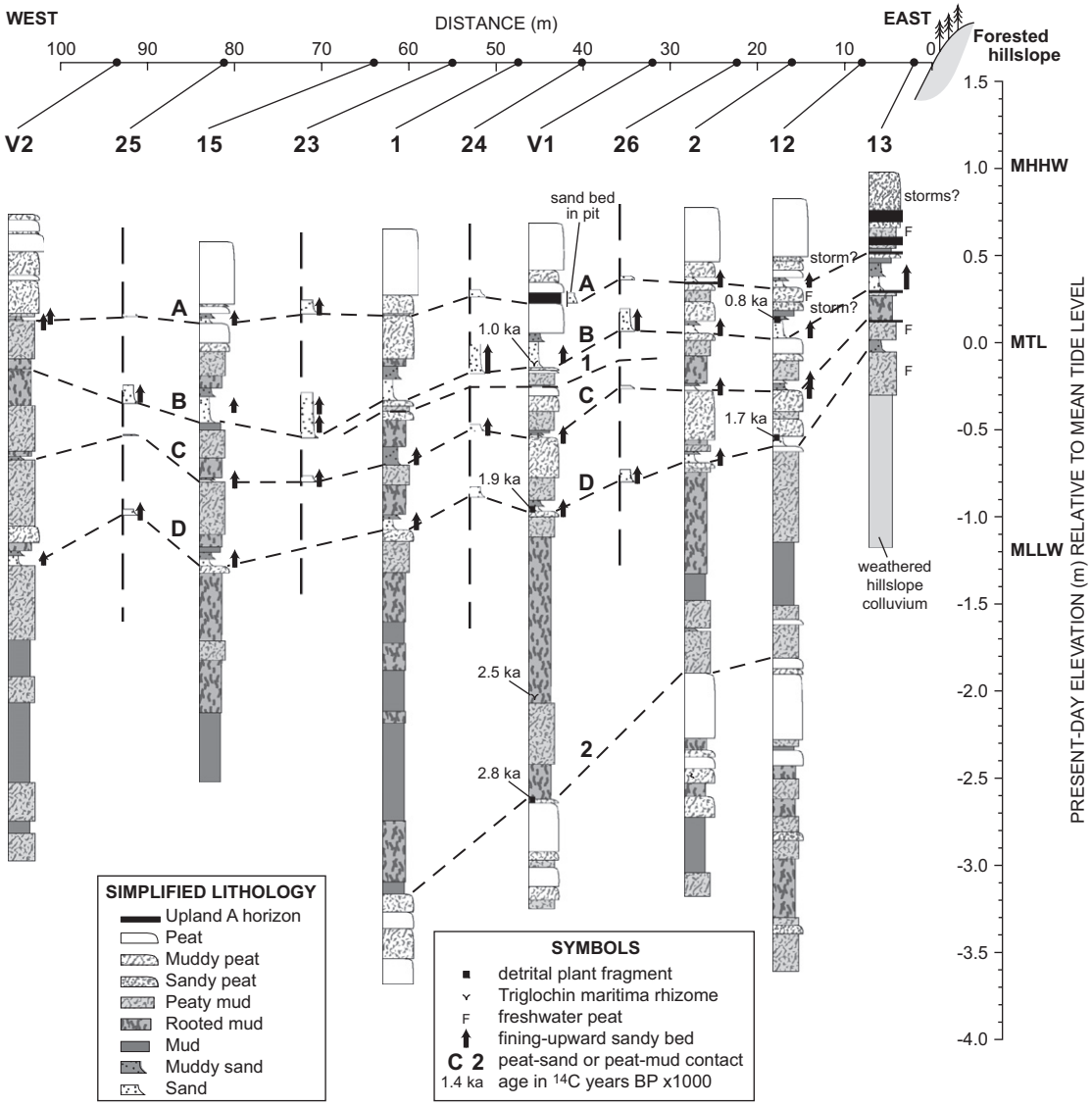

Fig. 4. Simplified lithology and correlation of contacts inferred to mark sudden rises in relative sea level caused by coseismic subsidence (sand beds and peat–sand contacts labeled A–D; peat–mud contacts labeled 1 and 2) in cores along transect 1. Vertical dashed lines mark cores whose nonsandy lithologies were not described in detail. Because sand A was not present at the unconformity at 0.47 m depth in core V1, an equivalent section containing sand A was sampled in a pit 2 m southwest of core V1 (Fig. 3). Core elevations (relative to the National Geodetic Vertical Datum of 1929) were determined by leveling (accuracy ±0.01 m) to a temporary benchmark. Benchmark elevation and tide levels (MTL, mean tide level; MHHW, mean higher high water; MLLW, mean lower low water) estimated as explained in text. Beds of sand too thin to map within sandy peat in cores 12 and 13 may have been carried into the high marsh during storm tides.

Upper sand sheet contacts are gradational over several millimeters or more. Root stirring of sheet sand into muddy or peaty beds above sheets is infrequent but more common in cores near the upland. Lower contacts of sheets are universally abrupt (0.5–1 mm) and commonly irregular or broken, probably reflecting minor erosion of underlying muddy sediment and rapid deposition of sand on well-vegetated soils in middle and high marshes. In a few cores, sand surrounds the stems of high-marsh plants. Where sheets overlie black, crumbly A horizons of the upper edge of the high marsh (Fig. 3), sand fills fractures and root casts in the A horizons (e.g., core 11, Fig. 2). In cores that lack one or more of the four sand sheets, we infer that abrupt, peat–mud contacts mark sudden marsh subsidence at the times sand sheets at similar stratigraphic levels were deposited and preserved on other parts of former marshes (Figs. 2B, 4, and 5).

Peterson and Darienzo (1996) discussed possible nontsunami depositional origins for the four sand sheets: river floods, storm tides, increases in regional sea level caused by ocean current anomalies, and changes in tide levels due to erosion of the sand spit at the mouth of the bay. Using hypersthene ratios in heavy mineral fractions to distinguish beach sand from river sand, these authors showed that percentages of beach sand in sandy beds and sand bed thickness decreased upriver in

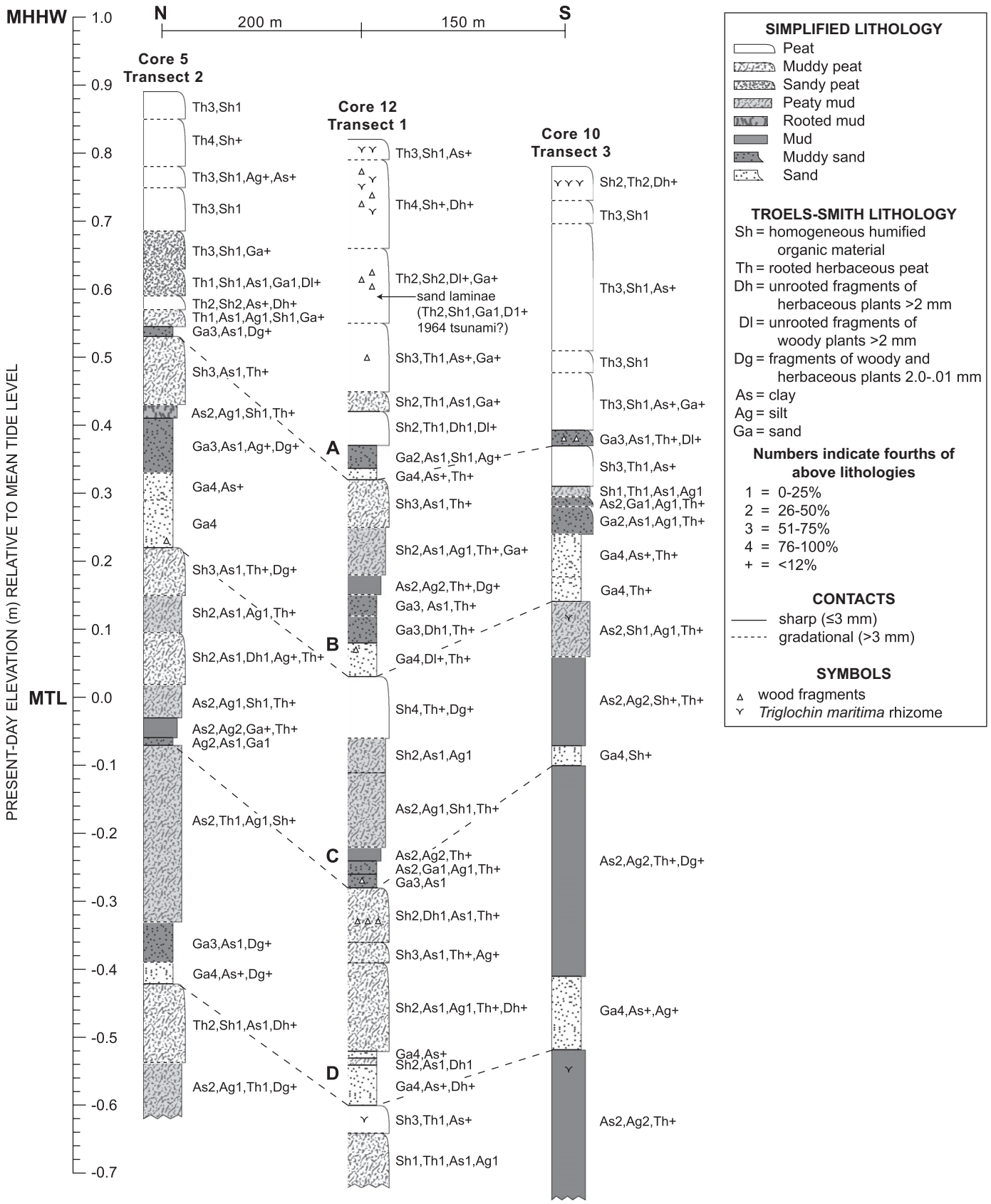

Fig. 5. Tidal lithofacies in one high-marsh core from each of the three core transects (Fig. 2B). Dashed lines correlate contacts among transects as in Fig. 4. Standard descriptions (Troels-Smith, 1955; Long et al., 1999) adjacent to cores show typical variability in core lithology. Core elevations measured relative to MTL at transect 1 as explained in text.

Please cite this article as: Nelson, A.R., et al., Great-earthquake paleogeodesy and tsunamis of the past 2000 years at Alsea Bay, central Oregon coast, USA. Quaternary Science Reviews (2008), doi:10.1016/j.quascirev.2008.01.001

Table 1
Thickness of four sand sheets beneath marshes in eastern Alsea Bay[a]

Thickness (mm)	Sand A	Sand B	Sand C	Sand D
Upper muddy sand				
Maximum	40	60	23	51
Mean	19±11 (6)	33±33 (17)	23±18 (13)	24±12 (9)
Lower clean sand				
Maximum	126	265	35	106
Mean	41±31 (18)	128±72 (29)	27±15 (13)	51±28 (21)
Total bed				
Maximum	126	265	45	106
Mean	44±32 (35)	145±75 (41)	32±15 (27)	67±35 (27)

Number of cores (42 total) in which measurements were made in parentheses.
[a]In many cores, an upper muddy sand bed overlies a lower clean sand bed. Mean shown at 1σ.

four cores spanning 3 km of Alsea River marshes. Current velocities resulting from storm tides or tidal cycles following sea-level changes are probably insufficient to transport sand this distance inland. And because decelerating river-flood currents are unlikely to deposit seaward-thickening sand beds, deposition by tsunamis remains the best explanation for the sand sheets (Peterson and Darienzo, 1996).

Sedimentary structures in selected cores are evidence for waning or variable current strength—a diagnostic characteristic of tsunami deposits (Nanayama et al., 2000; Clague et al., 2000b; Tuttle et al., 2004; Bourgeois et al., 2006; Morton et al., 2007). Where beds are >20 mm thick, most sand fines upward from fine-to-very-fine sand or from very fine sand to muddy sand. However, in a few cores penetrating sheets A, B, and D, the coarsest sand lies near the middle of the bed. About 5% of cores show indistinct laminae a few millimeters thick in the upper parts of beds. For example, in core 11 (Fig. 2), three laminae of couplets of fine sand and muddy very-fine sand, 2–3 mm thick, indicate rapidly changing flow regimes during the deposition of sheet A. Evidence for two or more distinct pulses of sand deposition is clear only for sheet B, where >100-mm-thick sandy beds in 12 of the 44 cores contain two distinctly graded beds, some with small mud or peat clasts near the base of beds. Clasts and laminae of muddy sand 3–5-mm thick between thicker beds of clean fine sand are evidence that sheet B in cores 10, 11, and 23 (Figs. 2 and 4) records two distinct pulses of deposition. For other sand sheets, only one or two cores show grading distinct enough to reflect multiple pulses of deposition.

Diatom and foraminiferal assemblages in the sand sheets are also consistent with deposition by tsunamis. As in all our core samples, the most abundant diatom taxa in sandy samples (4–69%) is *Paralia sulcata*, a decay-resistant, tychoplanktonic, marine-to-brackish species whose chain-like growth form ensures its wide dispersal (Crawford, 1979; Sawai et al., 2005). Diatoms typical of sandy tide flats, such as *Planothidium delicatulum*, *Dimeregramma minor*, and *Fallacia cryptolyra*, are the next most common species in sandy samples from core V1 (Fig. 6), but diatom valve concentrations are very low. Similar low-concentration diatom floras characterize some tsunami deposits elsewhere in Oregon and Washington (Hemphill-Haley, 1995, 1996) and Japan (Sawai, 2002; Soeda et al., 2004). The two foraminiferal samples from sheet B have so few foraminiferal tests (4–11 tests/mL; Fig. 7) that percentage data are not meaningful. A foraminiferal test of *Eggerella advena*, a subtidal species, in one of the samples is consistent with landward transport of subtidal sediment (e.g., Guilbault et al., 1996).

Laminae of fine-to-very-fine sand that are too thin (1–5 mm thick), discontinuous, or deformed to form extensive sheets occur within some peaty or muddy units, particularly in the upper 1 m of cores near the upper edge of the marsh. Sand in such laminae may have been transported by storm waves during extreme tides (e.g., Hemphill-Haley, 1995) or by tsunamis from distant subduction zones (e.g., Witter et al., 2001). The sandiest laminae, for example in the upper 0.25 m of cores 6, 12, and 13 (Figs. 2, 4, and 5), might have been deposited at the time of the great Alaskan earthquake of 1964, whose tsunami reached a height of 3.5 m in Yaquina Bay, 20 km north of Alsea Bay (Witter et al., 2001, their Fig. 4).

2.3. Other peat–mud contacts

We evaluated two other sharp peat–mud contacts, which lack sandy beds at similar stratigraphic levels: contact 1 just below sheet B at an elevation of −0.3 m and contact 2 at an elevation of −2.6 m (in core V1, Figs. 4, 6, and 7). Contact 1 abruptly (<1 mm) separates mud to slightly peaty mud from underlying rust-colored, high-marsh peat; a stratigraphy caused by a sudden increase in water level or sedimentation rate. Diatom and foraminiferal evidence is inconsistent in suggesting both a rise and fall of sea level across contact 1 (discussed in Section 4.5). Although contact 1 is distinct in two-thirds of cores near transect 1, we could not identify a similar contact in most cores on transects 2 and 3, or in outcrops south of transect 3 and along the main Alsea River channel. For this reason, contact 1 has too limited an extent to infer sudden, marsh-wide subsidence. The contact may record a small rapid change in tide levels, perhaps induced by changes in river channels or the configuration of the spit at the mouth of the bay, which affected tide levels in different parts of the Alsea Bay marshes in different ways.

The lithologic contrast across contact 2 in some cores (nos. 2, 4, 5, 7, 8, 12, 18, Figs. 2 and 3)—rooted mud over rust-colored, high-marsh peat—suggests a greater relative sea-level rise than across contact 1. Contact 2 may correlate with peat–mud contacts in cores along the Alsea River inferred by Peterson and Darienzo (1996) to record sudden subsidence during a great earthquake. But the contact is

Please cite this article as: Nelson, A.R., et al., Great-earthquake paleogeodesy and tsunamis of the past 2000 years at Alsea Bay, central Oregon coast, USA. Quaternary Science Reviews (2008), doi:10.1016/j.quascirev.2008.01.001

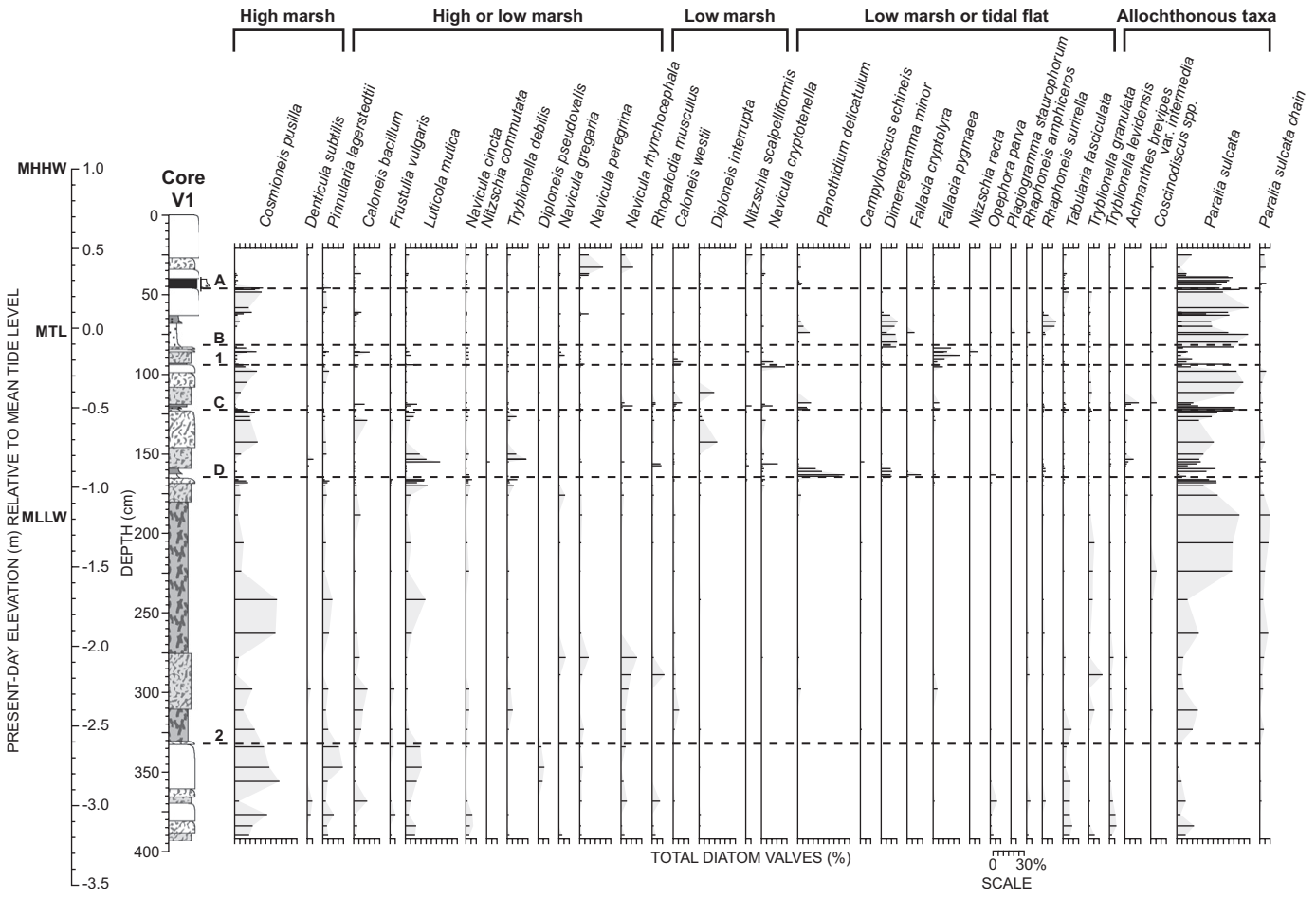

Fig. 6. Percentage of common species of diatoms in samples from core V1 grouped by preferred tidal environment and inferred allochthonous (transported) taxa. Lithologic patterns and contacts in core at left as in Fig. 4. All but three diatom samples <0.5 m deep are from the pit adjacent to core V1 (Figs. 3 and 9).

gradual (>10 mm) in some cores, lacks sand in all cores, has diatom evidence for only 0.21 ± 0.11 m of submergence (discussed in Section 4.5), and was identified in too few cores for us to be confident of its lateral extent. For these reasons, determining the regional significance of contact 2 will require its more detailed mapping at Alsea Bay, and identification and dating at sites to the north and south (e.g., Nelson et al., 1996a).

3. Radiocarbon dating and correlation

Most ^{14}C-dated fossils from the four sand sheets and contact 2 (Table 2) are detrital and so provide only maximum ages for the times when marshes were suddenly submerged and covered with sand or mud. In addition to stratigraphic context, the type of fossil, its likelihood of transport, and its resistance to decay were considered in selecting samples thought to predate ("close maximum") or postdate ("close minimum") sheets and contact 2 by no more than a few decades. Peterson and Darienzo's (1996, their Fig. 53) ^{14}C ages from peaty units in a core 1.2 km southeast of transect 3 are difficult to evaluate: the ages have large analytical errors and are on bulk peat, so the ages may predate marsh submergence and tsunamis by many hundreds of years (e.g., Nelson, 1992; Hamilton et al., 2005).

Nelson et al. (2006) correlated sand sheets A–D and contact 2 (labeled E in Fig. 2 of Nelson et al., 2006) with records of coseismic coastal subsidence and tsunamis to the north and south. Sheet A was almost certainly deposited by the tsunami from the great earthquake of 26 January AD 1700, which apparently ruptured much of the subduction zone (Satake et al., 2003; Atwater et al., 2005). Sheet B ages probably date a great earthquake and tsunami about 0.8 ka (ka, median of calibrated ^{14}C age in solar years BP rounded to nearest century; Table 2), younger than but within the large age uncertainties for tsunami beds in northern Oregon (Schlichting and Peterson, 2006) as well as the second most recent great earthquake in southwest Washington (Atwater et al., 2004a). If younger than the Washington earthquake, sheet B may record a tsunami from an earthquake rupture that broke only part of the subduction zone (Witter et al., 2003; Nelson et al., 2006). The only ages (two maximums) for sheet C show an age of <1.4–1.0 ka and, thus, a correlation with a great

Please cite this article as: Nelson, A.R., et al., Great-earthquake paleogeodesy and tsunamis of the past 2000 years at Alsea Bay, central Oregon coast, USA. Quaternary Science Reviews (2008), doi:10.1016/j.quascirev.2008.01.001

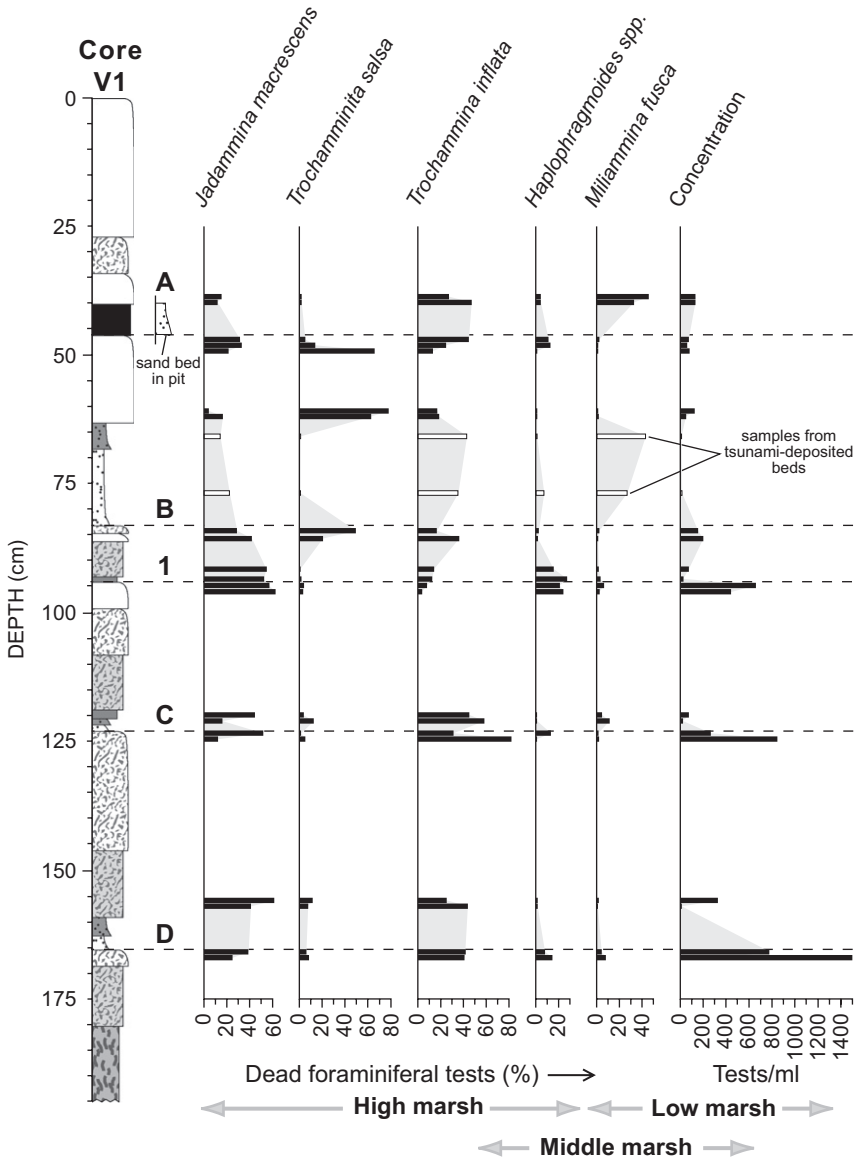

Fig. 7. Percentage of common species and concentration of foraminifera (number of tests/mL) in samples above and below key contacts in core V1. Lithologic patterns and contacts in core as in Fig. 4. Percentages for the two samples from sand B are shown by open bars to emphasize that these assemblages are transported. Foraminiferal samples from just above and below sand A are from the pit adjacent to core V1 (Figs. 3 and 9).

earthquake, precisely dated at 1.3–1.2 ka in southwest Washington (Atwater et al., 2004a), and less precisely at other sites in southern Oregon. Maximum and probable minimum ages for sheet D (Table 2) limit its age to the time of an earthquake with a similarly long rupture, dated at 1.6–1.5 ka in southwest Washington. Ages above and below contact 2 allow correlation with similar contacts of about this age inferred to record subsidence during a great earthquake about 2.9 ka (Atwater et al., 2004a; Nelson et al., 2006).

4. Microfossil-based paleogeodesy

Mapping patterns of coseismic deformation at Cascadia, as a means of estimating the rupture dimensions of plate-boundary earthquakes, requires quantitative measures of coastal vertical deformation. Where the elevational dependence of fossil assemblages has been defined through quantitative studies of modern plant and animal communities, precise estimates of elevation change, inferred from changes in relative sea-level, can be made (e.g., Hamilton and Shennan, 2005a). Measurements of the permanent submergence (relative sea-level rise) caused by coseismic subsidence come from studies of stratigraphic changes in macro- and microfossil assemblages across sharp peat–mud and peat–sand contacts (e.g., Nelson et al., 1996a; Shennan et al., 1996; Atwater and Hemphill-Haley, 1997). A succession of statistical methods has been applied to tidal microfossil datasets for reconstructing Cascadia relative elevation change (e.g., Whiting and McIntire, 1985; Hemphill-Haley, 1995; Nelson et al., 1996b; Shennan et al., 1998; Patterson et al., 2005), with results from transfer

Please cite this article as: Nelson, A.R., et al., Great-earthquake paleogeodesy and tsunamis of the past 2000 years at Alsea Bay, central Oregon coast, USA. Quaternary Science Reviews (2008), doi:10.1016/j.quascirev.2008.01.001

Table 2
Radiocarbon data for samples beneath a tidal marsh in eastern Alsea Bay[a]

Estimated age (cal yr BP)[b]	Calibrated age (cal yr BP at 2σ)[c]	Lab-reported age (^{14}C yr BP at 1σ)[d]	Provenance interpretation[e]	Radiocarbon lab no.	Core/ exposure[f]	Depth (m)	Description of dated material
Sand A							
<310–0	310–0	**170±80**	Close maximum	Beta-125097	E2	0.45	25 × 10-mm herb flower bud lying 5 mm above sand–peat contact
		205±50	Close maximum	CAMS-84710	P	0.51	Herb bud within peat at lower sand contact
Sand B							
850–700		420±40	Minimum	Beta-125096	E2	0.57	12 × 15-mm leathery rhizome frag 8 mm above overlying mud–peat contact
		590±60	Minimum	CAMS-84712	P	0.65	5 *Scirpus* sp., 2 *Carex* sp., and 3 other seed cases from 30 mm of peat above sand
	730–670	**755±30**[g]	Close minimum	OS-25274	C12	0.67	About 15 decayed *Picea stitchensis* leaves in fragments from within sand
		770±60[g]	Close minimum	CAMS-84711	P	0.66	Decayed rhizome in lower 10 mm of peat above sand
		1040±140	Maximum	OS-26199	E2	0.57	20 × 10-mm woody stem casing or bark from overlying mud–peat contact
	910–680	**855±40**	Close maximum	CAMS-84713	P	0.80	Two separate *Juncus* sp. rhizomes at lower sand contact
		1035±45	Maximum	AA-26604	V	0.84	Growth-position fibrous stem base of large herb at top of high-marsh peat
Sand C							
<1430–1050	1430–1050	**1360±90**	Maximum	OS-35705	P	1.08	Detrital piece of decayed rusty brown wood in middle of sand
		1520±95	Maximum	OS-35701	P	1.07	Detrital piece of woody herb horizontal near top of sand
Sand D							
1660–1450	1530–1340	**1530±40**[g]	Minimum	GX-26077	E2	1.41	20-mm-long rhizome 5 mm above overlying sand–mud contact
		1530±50[g]	Minimum	Beta-125099	E2	1.41	6-mm-long decayed rhizome 3 mm below overlying sand–mud contact
	1710–1540	**1690±50**	Close maximum	Beta-125095	C12	1.36	18 fragments of herb flower or bud 3 mm below top of sand
		1710±40	Maximum	OS-25275	E2	1.53	Cleanest 20-mm-long pieces of woody herb rooted in peat beneath sand
		1850±50	Maximum	Beta-125098	E2	1.53	15-mm-long pieces of *Triglochin maritime* and harpoon from lower contact
		1935±45	Maximum	AA-26603	V	1.66	Decayed fragments of stems, leaves, and roots of soft herbs
Contact 2							
	2760–2450	**2525±45**	Minimum	AA-26600	V	2.91	In-place stem base and leaves of *Triglochin maritima*; 40 cm above contact
	2960–2760	**2755±45**	Maximum	AA-26601	V	3.29	Stem base and rhizome of large herb at top of high-marsh peat
		2824±28[h]	Maximum	OS-58439	C10	2.69	20 × 15-mm immature cone of *Picea stitchensis*

[a]Ages are on unabraded fragments of flat-lying plant parts collected near the base or top of sandy units overlying high-marsh peat. Unless noted otherwise, samples are detrital and so ages are maximum ages for sediment at sample depth. Submitted samples weighed 2–45 mg and yielded ^{13}C values between −17.4‰ and −27.9‰.

[b]Best estimate of the age of tsunami-deposited sand and contact 2 in core V1 (Fig. 4), based on selected ages (in solar years; in third column) using the sequence analysis feature of the program OxCal (version 3.10; Bronk Ramsey, 1995, 2001; probability method). Sample ^{14}C ages selected on basis of quality of material dated and stratigraphic context. Estimates for sands A and C are maximum time intervals based on close maximum ages. Estimates for sands B and D are 2σ time intervals between close maximum and close minimum ages (or means of two ages with the same provenance interpretation in third column) calculated using OxCal and rounded to nearest decade.

[c]Calibrated ages calculated from selected ages in bold in third column. Ages in solar years calculated using OxCal (version 3.10; Bronk Ramsey, 1995, 2001; probability method) with the INTCAL04 atmospheric dataset (Reimer et al., 2004). NOSAMS' (OS), Tucson's (AA), and Lawrence Livermore's (CAMS) results from the Third International Radiocarbon Comparison show minimal offset from comparison means (e.g., Elder et al., 1998) suggesting that no additional interlaboratory variance (error multiplier; e.g., Taylor et al., 1996) is required for calibration. Calibrated ages show time intervals of >95% probability distribution at 2σ. Ages to the left of two consecutive ages in bold in third column are calibrated from the mean of the two ages.

[d]Accelerator mass spectrometer (AMS) age reported by radiocarbon laboratory. Quoted errors for ages are the larger of counting error or target reproducibility error. Reported age of 755±30 ^{14}C yr BP from core C12 is the average of two ages on the same sample.

[e]Interpretation of the provenance, or stratigraphic context, of the dated sample relative to the time of great earthquakes and tsunamis. Maximum ages are on samples containing carbon judged to be older than the earthquake, minimum ages are on samples judged younger than the earthquake, and "close" ages are those on samples judged to contain carbon produced within a few decades of the earthquake.

[f]E, exposure; P, 1.5-m × 2-m × 1.5-m-deep pit; C, 25-mm-diameter gouge core; V, 70-mm-diameter vibrocore (Fig. 3).

[g]Rhizome probably grew after sand was deposited and so age is a minimum for sand deposition. *Picea* leaves may have been thrust into sand by a toppling tree.

[h]Mean of two ages on same sample.

Please cite this article as: Nelson, A.R., et al., Great-earthquake paleogeodesy and tsunamis of the past 2000 years at Alsea Bay, central Oregon coast, USA. Quaternary Science Reviews (2008), doi:10.1016/j.quascirev.2008.01.001

function analysis being the most objective and precise (e.g., Guilbault et al., 1995, 1996; Hughes et al., 2002a; Sabean, 2004).

Transfer function analysis of microfossil assemblages has been widely used to reconstruct relative sea-level changes recorded in tidal sediment (e.g., Horton et al., 1999b; Shennan et al., 1999; Zong and Horton, 1999; Gehrels, 2000; Gehrels et al., 2001; Sawai et al., 2004a; Horton and Edwards, 2006; Shennan and Hamilton, 2006). A training set of modern microfossil data, from transects extending from tide flat to forested upland, is analyzed to determine relations among the abundances of species and the independent variable elevation (relative to MTL). The relations are then used to reconstruct past changes in elevation using fossil assemblages in cores, assuming no change in sea level. Transfer functions have the substantial advantage over earlier quantitative and semi-quantitative methods (e.g., Nelson and Kashima, 1993; Hemphill-Haley, 1995; Kelsey et al., 2002) of continuously modeling sea-level change (including sample-specific errors) throughout earthquake cycles (Long and Shennan, 1994; Zong et al., 2003; Sabean, 2004; Hamilton and Shennan, 2005b).

At Alsea Bay we apply transfer function analysis to two complementary microfossil groups—diatoms and foraminifera—to estimate the amount of submergence at the times that sand sheets A–D and contacts 1 and 2 formed. Diatoms are small (10–200 μm), abundant, resistant to decay, and sensitive to tidal inundation and salinity, but are easily transported and so may be allochthonous (reworked). Foraminifera are large (50–2000 μm) and so less likely to be allochthonous, but are less resistant to decay and may be infaunal (burrow into sediment). There are many hundreds of common tidal diatom species, but only a few tens of common tidal foraminiferal species. Assemblages of both types of taxa may be modified by poorly understood ecologic and taphonomic processes (Goldstein and Watkins, 1999; Sawai, 2001; Patterson et al., 2004). Analysis of fossil assemblages from multiple microfossil groups reduces interpretive problems encountered when using only one group (e.g., Nelson et al., 1996b; Shennan et al., 1998; Gehrels et al., 2001; Hughes et al., 2002a; Patterson et al., 2005).

4.1. Diatom sampling and analysis

Modern and fossil samples counted for diatoms included 21 1-ml samples from 0 to 2 cm depth along transect 1 (modern samples 0–20 on Fig. 3) and 90 3–5-mm-thick samples from the upper 4 m of core V1 and two nearby hand-dug pits (Fig. 3; Table SD1). About 20 mg of dry sediment from each sample was cleaned with sodium hypochlorite solution, centrifuged in water, and dried on a slide (methods and autecology as described by Sawai, 2001). At least 300 diatom valves were counted under an oil-immersion microscope; fragments containing more than half a valve were included in the count. We identified 80 taxa in 34 genera in the modern samples and 148 taxa in 68 genera in the fossil samples. Sawai and Nagumo (2003) describe the taxonomy of and illustrate modern taxa of the Alsea Bay flora.

4.2. Foraminiferal sampling and analysis

Modern samples counted for foraminifera included 20 20-ml samples from 0 to 2 cm depth along transect 1 (samples 1–20 on Fig. 3) and 20-ml samples from 2 to 10 cm depth from 9 of these sites (Fig. 8). Fossil samples included 23 10-mm-thick, 10-ml samples from core V1 and the pit 2 m from it (Fig. 3; Table SD2). Standard preparation methods included staining of modern samples with rose bengal mixed with methanol to determine the foraminifers living at the time of collection, wet sieving at 63 μm to isolate the sand fraction, and careful decanting of organic material to facilitate counting and identification. Representative samples containing 250–400 foraminifers were obtained by wet splitting and counted in a methanol and water solution. Except for one modern sample from the upland (total of 28 tests), one from the high marsh (16 tests), and three fossil samples from tsunami-deposited sand (7–57 tests), we counted >100 living plus dead foraminifers in each sample. We identified seven species in the modern samples and 10 tidal species in the fossil samples; small numbers of planktonic species in four fossil samples were excluded from the total count. All comparisons of modern assemblages with fossil assemblages used only percent dead foraminifera (living foraminifers excluded) because dead assemblages best reflect the long-term effects of taphonomic processes (Horton, 1999; Murray, 2000; Patterson et al., 2005). Counts of dead tests ranged from 35 to 420 (mean 165) in the modern samples to 73–571 (mean 228) in fossil samples.

Over the past two decades, studies of tidal foraminifers have demonstrated important taphonomic effects on foraminiferal assemblages as deep as 60 cm below the surface of some tidal marshes. Variability in the spatial distribution of assemblages leads some investigators to conclude that surface samples (1-cm thick) of foraminifera are not necessarily representative of tidal environments. Elevational dependence of fossil assemblages may be obscured by seasonal, inter-seasonal, and interannual differences in assemblages due to ecologic or diagenetic factors, such as changes in pore-water chemistry, as well as by infaunal migration of some species to depths of tens of centimeters (Scott and Leckie, 1990; de Rijk and Troelstra, 1997; Ozarko et al., 1997; Goldstein and Watkins, 1999; Patterson et al., 1999, 2004; Hippensteel et al., 2002; Horton and Edwards, 2003; Martin et al., 2003). Some advocate analysis of 10-cm-thick samples to capture infaunal as well as epifaunal species (Ozarko et al., 1997; Goldstein and Watkins, 1999; Patterson et al., 1999). But analysis of 10-cm-thick samples obscures sea-level changes spanning less than centuries (in all but the highest sedimentation rate samples), and so would make foraminiferal study of coseismically subsided marsh beds in cores,

Please cite this article as: Nelson, A.R., et al., Great-earthquake paleogeodesy and tsunamis of the past 2000 years at Alsea Bay, central Oregon coast, USA. Quaternary Science Reviews (2008), doi:10.1016/j.quascirev.2008.01.001

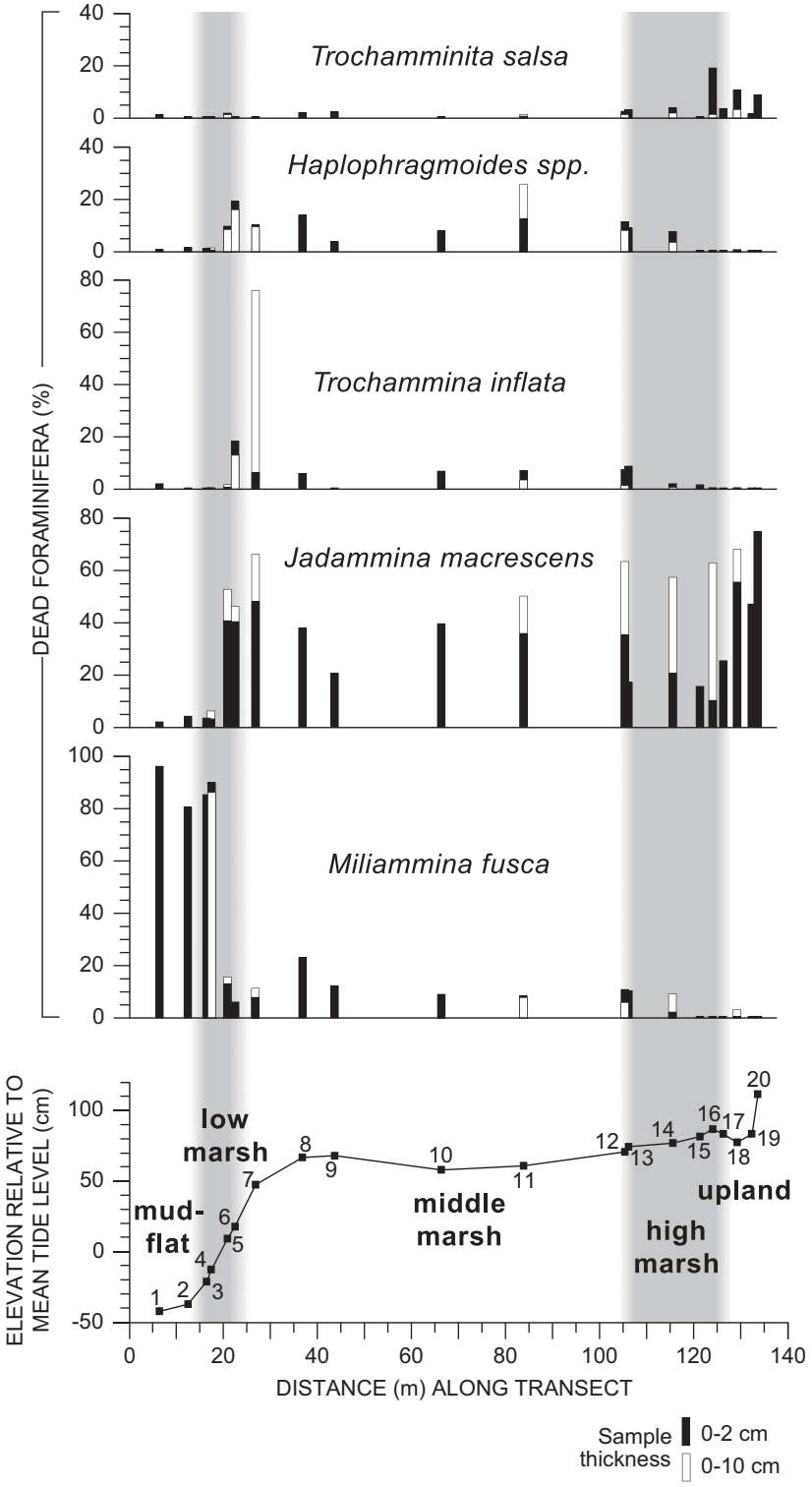

Fig. 8. Percent of common foraminiferal species (>2% of dead assemblage) in assemblages from a depth of 0–2 cm, compared with assemblages from a depth of 0–10 cm, along transect 1. Elevation of samples relative to tidal vegetational zones (alternating white and gray columns) identified based on vascular plant communities is shown at bottom of diagram; zones boundaries are 0.6–0.9 m lower than those reported by Peterson and Darienzo (1996).

which are typically 5–30 mm thick, of little use. Other studies have found only modest effects on assemblage proportions due to infaunal migration and diagenesis, and have successfully used surface samples as good modern analogs in reconstructing sea-level change from fossil samples (Horton, 1999; Patterson et al., 2004; Sabean, 2004; Horton and Edwards, 2006).

To test for the effect of infaunal migration and diagenesis at Alsea Bay, we combined percentage and concentration data from depths of 0–2 and 2–10 cm for

Please cite this article as: Nelson, A.R., et al., Great-earthquake paleogeodesy and tsunamis of the past 2000 years at Alsea Bay, central Oregon coast, USA. Quaternary Science Reviews (2008), doi:10.1016/j.quascirev.2008.01.001

paired samples at nine locations along transect 1 to obtain species percentages for 20-ml samples spanning a depth range of 0–10 cm (Fig. 8). Comparison of dead species percentages from depths of 0–2 cm with those from depths of 0–10 cm shows that infaunal migration affects—but probably does not seriously compromise—paleoenvironmental reconstruction using foraminifera from core V1 (Fig. 8). Greater percentages of *Jadammina macrescens* in deep samples at three high-marsh stations probably reflect the infaunal migration documented for this species in several studies cited above; percentages of the epifaunal species *Miliammina fusca* are similar in samples from both depth ranges. Q-mode cluster analysis (software of Hammer et al., 2006) of 0–2 and 0–10-cm data yielded similar clusters (e.g., Patterson et al., 2004).

4.3. Transfer function analysis

We follow recent studies (e.g., Zong and Horton, 1999; Gehrels et al., 2001; Hughes et al., 2002a; Horton and Edwards, 2003; Sawai et al., 2004a, b; Hamilton and Shennan, 2005a; Horton and Edwards, 2006) in using the statistical methods reviewed by Birks (1995) with the software of Juggins (2003) to compare various transfer function models for reconstructing elevation change (relative to MTL) from diatom and foraminiferal data (Fig. 9). The method develops relations among species percentages in modern assemblages and elevation that are then used to estimate elevation for fossil assemblages from core V1 (and for 28 samples from the pits next to cores V1 and 12, Figs. 3, 9, and 10).

To begin we use the modern analog technique (weighted modern analog of Juggins, 2003) to learn which of the fossil samples from the core have good-analog assemblages in the modern samples from transect 1. Transfer function results for fossil samples that have poor analogs in the modern training set are suspect (Birks, 1995; e.g., Hughes et al., 2002a; Hamilton and Shennan, 2005a). Unfortunately, only 6 of 90 diatom samples from the core and none of the 23 foraminiferal samples have good analogs using the 5% minimum dissimilarity coefficient criteria proposed by Hamilton and Shennan (2005a). The lack of good analogs is probably due to the small number (20) of modern samples from Alsea Bay, taphonomic problems in comparing modern with fossil foraminiferal assemblages, and the substantial percentages of some diatom species in the modern samples not found in the fossil samples (Table SD1).

To deal with insufficient modern analogs we expand the modern data sets (e.g., Horton and Edwards, 2005). To the Alsea Bay foraminiferal training set we add all but five low-concentration samples (<11 tests/ml) from the three southern Oregon transects reported by Jennings and Nelson (1992). The tidal marsh settings of the additional transect sites are much like the Alsea Bay marsh and methods of sample preparation and analysis are identical. *Trochamminita salsa* is an important foraminiferal species in some Alsea Bay core samples (Fig. 7), but because we did not recognize *T. salsa* during counting of the three transects in 1987 we did not use this species in the transfer function analysis (Table SD2; e.g., Jennings et al., 1995). The resulting seven foraminiferal species make up >97% of dead tests in modern assemblages and >93% of the core assemblage. Excluding small percentages of calcareous species in the fossil samples from the analysis reduces differences between core and modern samples due to possible dissolution of calcareous tests (Edwards and Horton, 2000). Because tidal range differs by 0–0.3 m at the four foraminiferal transect sites, we normalize sample elevations using a standardized water level index (e.g., Horton et al., 1999a; Gehrels, 2000; Hamilton and Shennan, 2005a).

To the Alsea Bay diatom training set we add percentage data from 39 modern tidal samples from four sites in southern Puget Sound (Sherrod, 2001). The new modern training set includes species with values of >3% in any sample for a total of 104 species, 48 of which occur in core samples. Although the sheltered Puget Sound environments differ in some ways from the outer coastal estuarine site at Alsea Bay, comparable modern diatom data is not available from other Oregon estuaries. Sample preparation procedures and taxonomy used by Sherrod (2001) are similar to those of Sawai and Nagumo (2003) at Alsea Bay. As with the foraminiferal samples, we normalize elevations of the diatom samples to account for differences in tidal range.

Transfer function models for the expanded diatom and foraminiferal data sets use partial least squares weighted-averaging regression with inverse deshrinking and bootstrapping, as explained in Birks (1995), Gehrels et al. (2001), Hughes et al. (2002a), Sawai et al. (2004a), Horton and Edwards (2006), and references therein. Detrended canonical correspondence analysis confirms that unimodal statistics, as implemented by this type of regression, are appropriate for both data sets (gradient lengths: diatoms, 2.4; foraminifera, 3.0; Birks, 1995). We use low values of the root mean square error of prediction (RMSEP) and high values of the coefficient of determination (r^2) to select the transfer function models most effective in reconstructing past elevations (Birks, 1995; Juggins, 2003; e.g., Horton et al., 1999a; Hamilton and Shennan, 2005a). For each data set, samples with residuals (normalized observed elevation minus normalized predicted elevation) greater than 1σ of normalized elevation are not used in the models (three foraminiferal samples, two diatom samples). Plots of residuals help us eliminate an additional outlier from the modern foraminiferal data set and two from the diatom data set. Rerunning the modern analog technique on the expanded training sets with outliers removed gives much improved results: 56 of 90 diatom samples from the core have good modern analogs, whereas 16 of 23 foraminiferal samples have good analogs (Fig. 9). For the final models used to reconstruct elevation (Figs. 9 and 10), coefficients of determination are $r^2 = 0.88$ for diatoms

Please cite this article as: Nelson, A.R., et al., Great-earthquake paleogeodesy and tsunamis of the past 2000 years at Alsea Bay, central Oregon coast, USA. Quaternary Science Reviews (2008), doi:10.1016/j.quascirev.2008.01.001

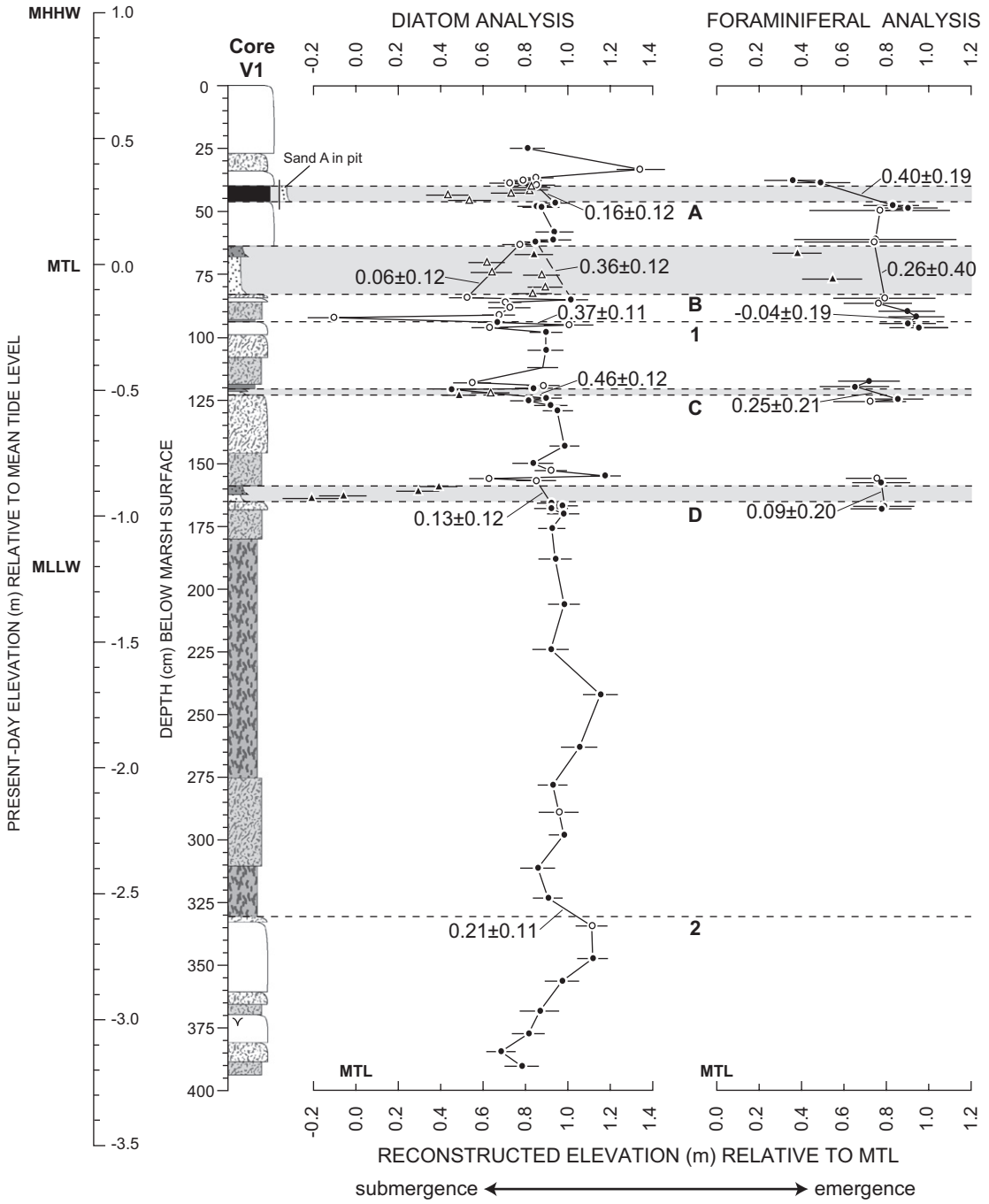

Fig. 9. Reconstructed elevation (relative to MTL at transect 1) at the site of core V1 (Figs. 2 and 3). Lithologic patterns and contacts as in Fig. 4. Because sand A was not present at the unconformity at 0.47 m depth in core V1, sand A as exposed in the pit 2 m to the southwest is shown next to the core. Transfer functions use modern diatom and foraminiferal species percentages from four transects in southern Oregon (Jennings and Nelson, 1992; this study) and fossil assemblage percentages from the core and adjacent pit (Figs. 6–8, 10; Tables SD1 and SD2). Transfer function values above 0.5 m depth for all foraminifera samples and all but 3 of the 15 diatom samples are also from the pit (where sand A was present) rather than from the core. The amount of subsidence across sand sheets A–D (including sand thickness), and contacts 1 and 2, are indicated by the bold numbers (errors calculated from differenced transfer function values). Samples from tsunami-deposited sandy beds (triangles not connected with line segments) are not meaningful in elevation reconstruction. Open symbols shows samples that do not have a good analog in the modern data set. Dashed line within sand B shows an alternative measure of subsidence using good-analog samples.

(RMSEP = 0.15 m) and $r^2 = 0.78$ for foraminifera (RMSEP = 0.27 m). Combining diatom and foraminiferal data sets (e.g., Gehrels et al., 2001; Patterson et al., 2005) is not an option because the core was sampled separately at different levels for diatoms and foraminifera.

4.4. Coseismic elevation changes

Reconstruction of changes in elevation at the site of core V1 with the diatom and foraminiferal transfer functions include modest subsidence (0.3 ± 0.3 m) during the past

Please cite this article as: Nelson, A.R., et al., Great-earthquake paleogeodesy and tsunamis of the past 2000 years at Alsea Bay, central Oregon coast, USA. Quaternary Science Reviews (2008), doi:10.1016/j.quascirev.2008.01.001

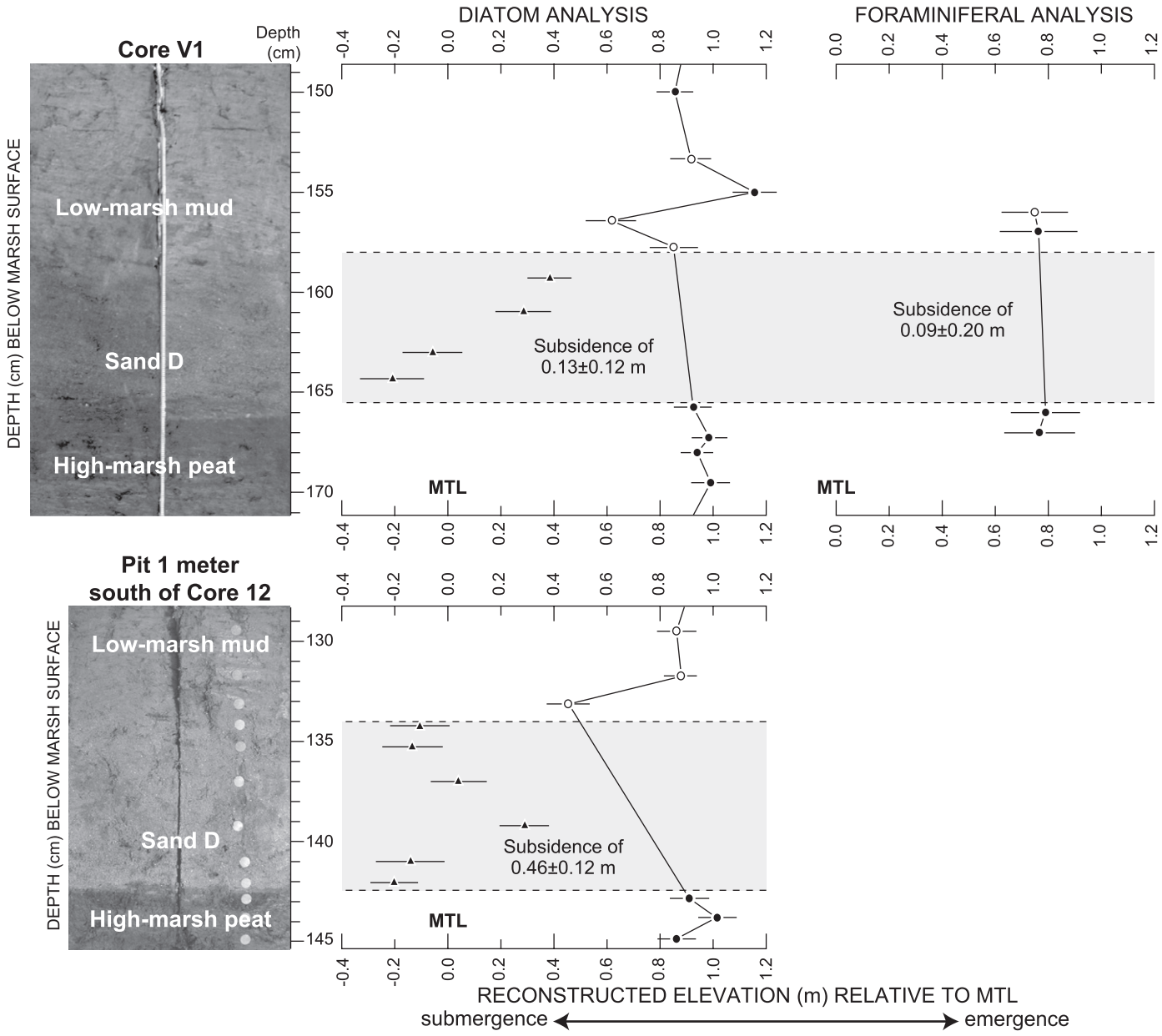

Fig. 10. Detail of elevation changes reconstructed with transfer functions about the time sand D was deposited. Results for diatom samples from the pit 1 m south of core 12 (Fig. 3) are shown below results from core V1. Symbols as in Fig. 9.

four great earthquakes at Alsea Bay, but interpretation is complicated by the 30–38% of potentially unreliable transfer function values from samples with poor modern analogs (Fig. 9). Transfer function values for samples from tsunami-deposited sandy beds (triangles on Fig. 9) are not meaningful in elevation reconstructions. For example, abundant commonly allochthonous diatom taxa, such as *Paralia sulcata* and the sandy tide-flat/subtidal species *Dimeregramma minor* (Fig. 6), show that diatom assemblages in sandy samples are unrelated to tide levels. Because the modest elevation changes resulting from the transfer function analysis are no greater than the changes produced by late Holocene relative sea-level changes common to nontectonic coasts, the seismic land-level changes we infer below are easily confused with nonseismic sea-level changes (e.g., Nelson et al., 1996a; Shennan et al., 1998; Hamilton and Shennan, 2005a). However, at Alsea Bay the regionally correlative ^{14}C ages (Table 2; Nelson et al., 2006) for the tsunami-deposited sheets of sand on contacts A–D support our inference that the contacts coincide with Cascadia plate-boundary earthquakes and so record coseismic changes.

At the deposition time of sand sheet A (AD 1700), foraminifera show 0.40 ± 0.19 m of subsidence whereas diatoms yield only 0.16 ± 0.12 m, even if the thickness (0.06 m) of tsunami-deposited sand is considered in reconstructing postseismic elevation (Fig. 9; e.g., Guilbault et al., 1996; Hughes et al., 2002b). However, poor-analog

Please cite this article as: Nelson, A.R., et al., Great-earthquake paleogeodesy and tsunamis of the past 2000 years at Alsea Bay, central Oregon coast, USA. Quaternary Science Reviews (2008), doi:10.1016/j.quascirev.2008.01.001

samples—as at the top of sand A and bounding sand B—make some subsidence estimates unreliable. Values for good-analog diatom samples above sand B suggest that deposition of this 0.2-m-thick bed did not raise the level of the marsh above the pre-earthquake level, which implies subsidence of at least 0.2 m. Ignoring the poor-analog diatom samples immediately above and below sand B gives a measure of subsidence of 0.36 ± 0.12 m across the bed (dashed line in sand B on Fig. 9). The foraminiferal samples from this part of the core have poor analogs because they contain abundant *Trochammina salsa*, which is absent or present in much lower proportions in the modern samples (Table SD2). Assuming the diatom assemblage in the sample at the upper contact of sand C (1.21 m depth) is largely autochthonous (unreworked), diatom assemblages yield almost twice as much subsidence for the earthquake of about 1.3 ka as foraminiferal assemblages (0.46 m vs. 0.25 m, Fig. 9), although errors on reconstructions overlap. Similarly, for the earthquake of about 1.6 ka, a mix of good-analog and poor-analog foraminiferal and diatom samples yield less subsidence (about 0.1 ± 0.2 m) across sand D in core V1, whereas diatom samples across the same sand in the pit 1 m from core 12 suggest three times this amount (Fig. 10).

Such variation in transfer function values emphasizes the uncertainty in poor-analog sample values and shows greater variability than implied by sample-specific function errors. These results, in turn, emphasize the importance of acquiring large modern data sets that sample a full range of tidal environments and fossil analyses from multiple sites in the same marsh, preferably using multiple microfossil groups (e.g., Nelson et al., 1996b; Shennan et al., 1996; Hamilton and Shennan, 2005a; Patterson et al., 2005), for reconstructing land-level movement during earthquake cycles.

4.5. Nonseismic elevation change

Are the transfer function reconstructions reasonable measures of coastal subsidence due to plate-boundary slip during great earthquakes, or do they fail, as postulated by Hemphill-Haley (1995), to include additional components of nonseismic land- and sea-level change, such as changes in tidal range, coseismic sediment compaction, and postseismic uplift or subsidence of the coast (Leonard et al., 2004)? The broad, shallow configuration of Alsea Bay and the gentle slope of present and former marshes on its eastern shore probably resulted in minimal changes in tidal range over the past 2000 years (e.g., Hughes et al., 2002a). Because well-compacted Pleistocene sediment probably lies <7 m beneath core V1 and extensive river channel exposures show no evidence of widespread liquefaction, compaction of core sediments is probably limited to the ubiquitous, gradual compaction of muddy, organic-rich sequences on many coasts (e.g., Guilbault et al., 1995; Allen, 2000; Shennan and Horton, 2002). In any case, compaction only increases apparent coastal subsidence (Horton and Edwards, 2006).

Our most reliable reconstructions imply that postseismic uplift at Alsea Bay caused by slip on deep parts of the plate boundary and (or) viscoelastic stress relaxation (Hyndman et al., 2005; e.g., Hu et al., 2004; Sawai et al., 2004b; Uchida et al., 2004; Chlieh et al., 2007; Wang, 2007) may be almost as large as coseismic subsidence (Fig. 9). Geophysical modeling of plate-boundary deformation shows that postseismic deep fault slip would increase subsidence at central Oregon sites, 100 km inland from the Cascadia deformation front (Fig. 1), whereas uplift from viscoelastic relaxation would reduce it (Hyndman et al., 2005; Wang, 2007). As did Guilbault et al. (1996), Hughes et al. (2002a), and Hamilton and Shennan (2005a), we infer that transfer function values differenced across contacts in core V1 include postseismic effects occurring within a few years of earthquakes. Because tsunamis deposited the four sand sheets on subsided Alsea Bay marshes within minutes to hours following great earthquakes, the overlying muddy beds (into which all the sheets grade, e.g., Fig. 10) probably began accumulating within hours to days of an earthquake. High rates of apparent uplift measured from good-analog samples immediately above sand beds C and D support this assumption. Differenced post-tsunami transfer function values give ratios of elevation increase/sediment thickness just above sand C of 32 (390 mm of elevation increase over 12 mm of sediment thickness; diatoms) and 10 (foraminifera), and of 30 (diatoms) above sand D in the pit at core 12. Poor-analog samples make similar calculations for other beds unreliable. Hughes et al. (2002b) also inferred rapid uplift from similar ratios obtained with transfer functions on fossil pollen deposited on Vancouver Island following the AD 1700 earthquake. Although we cannot rule out unrecognized postseismic movements within weeks following great earthquakes (Hyndman et al., 2005), the few reliable Alsea Bay reconstructions suggest 0.4 ± 0.2 m of coseismic subsidence followed by rapid recovery in the first few decades following the earthquake. Wang (2007) calls on stress relaxation to explain similar recovery following great earthquakes of the past century in other subduction zones.

Other investigators have reported microfossil evidence of slow sea-level rise that is increasingly interpreted as decades of slight subsidence prior to great plate-boundary earthquakes, as predicted by models of the earthquake deformation cycle in subduction zones (e.g., Long and Shennan, 1998; Shennan et al., 1998, 1999; Zong et al., 2003; Hamilton et al., 2005; Hawkes et al., 2005; Shennan and Hamilton, 2006). At Alsea Bay, our sampling is too limited and transfer functions too imprecise to argue for or against preseismic subsidence. Small and inconsistent apparent decreases in relative elevation beneath the sand sheets (e.g., Fig. 10) may reflect mixing of taxa from assemblages above the contacts or small local-to-regional accelerations in sea-level rise caused by nontectonic processes (Fig. 6; e.g., Nelson et al., 1996b, p. 151; Hamilton et al., 2005).

Please cite this article as: Nelson, A.R., et al., Great-earthquake paleogeodesy and tsunamis of the past 2000 years at Alsea Bay, central Oregon coast, USA. Quaternary Science Reviews (2008), doi:10.1016/j.quascirev.2008.01.001

Transfer functions are inconsistent in yielding both subsidence (diatoms, 0.37 ± 0.11 m) and uplift (foraminifera, -0.04 ± 0.19 m) across contact 1. Across contact 2, diatoms show subsidence of 0.21 ± 0.11 m, but even this change is less than some reconstructed changes where core lithology is uniform or changes gradually, for example near 2.4 m depth (Fig. 9). For the changes across contacts 1 and 2, our data cannot distinguish between coseismic relative sea-level changes and local-to-regional sea-level changes unrelated to land-level movements during earthquake cycles (e.g., Nelson et al., 1998; Allen, 2000; Hamilton and Shennan, 2005b).

5. Great-earthquake rupture dimensions and magnitudes

Unless substantial postseismic rebound was too rapid to be recorded, reconstructions of land-level change at Alsea Bay indicate modest (0.4 ± 0.2 m) coseismic subsidence inconsistent with wide plate-boundary ruptures extending well inland of the coast (e.g., Hyndman and Wang, 1995). Leonard et al. (2004) compared qualitative to semi-quantitative tidal wetland evidence of coseismic subsidence with amounts of subsidence predicted by the elastic dislocation models of Flück et al. (1997) and Wang et al. (2003) for great earthquakes with 800 and 550-yr strain cycles and variable slip (Fig. 11). A compilation of less detailed evidence for pre-AD-1700 great earthquakes gave almost identical results for the central Oregon coast (Hyndman et al., 2005). Our estimates of coseismic subsidence fall in the middle range of Leonard et al.'s (2004) mean subsidence values near Alsea Bay. The estimates encompass the 550 and 800-yr strain cycle models (A, Fig. 11) and best fit modeled earthquakes with <30 m of plate-boundary slip (B, Fig. 11).

Coseismic subsidence estimates from other statistically supported microfossil studies in central Cascadia are mostly <1 m (Fig. 11), and best fit models of largely offshore coseismic rupture. For example, recent transfer function results using logarithms of foraminiferal species concentrations record only 0.6–1.0 m of subsidence during the past four plate-boundary earthquake cycles in northern Willapa Bay (Fig. 1), although Sabean (2004) interprets these as minimum values. At Coos Bay, analysis of foraminiferal data gathered in the 1980s (Nelson et al., 1996b) with the same transfer function (modern training set) used here (87% of Coos Bay fossil samples have good modern analogs) yields subsidence of 0.7 ± 0.3 m during the two largest earthquakes of the past 2000 years (Fig. 11). Current interseismic GPS data and historical tide gauge and leveling-line data are also consistent with the locked portion of the plate boundary, inferred to coincide with the rupture zone, lying offshore in central Oregon (Wang et al., 2003; Yoshioka et al., 2005; Schmidt et al., 2007). Wells et al. (2003) reached similar conclusions about the inland extent of ruptures at Cascadia through a comparison of historical great-earthquake rupture zones and forearc basin distribution in other subduction zones.

Narrow, offshore rupture zones in central Oregon might reflect plate-boundary earthquakes of variable dimensions and magnitudes. Long narrow ruptures, with unusually large length-to-width ratios (>10), imply earthquakes near magnitude 9. Precise radiocarbon dating and tree-ring records from earthquake-killed trees suggest a rupture of >900 km for the AD 1700 earthquake (Atwater et al., 2005; Nelson et al., 2006) and inversions of reconstructions of the accompanying tsunami on Japan's east coast yield magnitudes in line with such a rupture length (M8.7–9.2; Satake et al., 2003). For some earlier great earthquakes at Alsea Bay, subsidence of 0.4 ± 0.2 m might be more easily explained by ruptures of more limited north–south extent and lower magnitude (e.g., Nelson and Personius, 1996; Satake et al., 2003, their Fig. 8; Witter et al., 2003; Nelson et al., 2006; Satake and Atwater, 2007). Earthquakes whose rupture widths decreased as they approached Alsea Bay from the north or south, or earthquakes in central Oregon with modest rupture areas (low M8 range) are also consistent with 0.4 ± 0.2 m of coseismic subsidence.

Such variability in rupture dimensions might explain differences in coastal subsidence from one earthquake to the next. Incomplete strain release during plate-boundary earthquakes, as postulated to explain earthquakes of variable magnitude at other subduction zones (e.g., Atwater et al., 2004b; Natawidjaja et al., 2004; Cisternas et al., 2005; Briggs et al., 2006), is another likely explanation for differences in coseismic subsidence (Hyndman et al., 2005). For example, if the 0.2 ± 0.2 m of subsidence measured across sand D in the core (average of three values) is accurate (Figs. 9 and 10), the great earthquake of about 1.6 ka could have released less accumulated plate-boundary strain than at least two of three later earthquakes. In the case of the 1.6-ka earthquake, however, the wide distribution of evidence for substantial coseismic subsidence ($\sim$1 m) about 1.6 ka is less consistent with a partial-strain-release earthquake of M8 than with an M9 earthquake that ruptured much of the subduction zone (Nelson et al., 1996a; Fig. 11).

6. Conclusions

Four sheets of tsunami-deposited sand interrupt the upper 2 m of tidal peat and mud beneath marshes fringing the eastern shore of Alsea Bay. The sheets have characteristics typical of tsunami deposits and ^{14}C ages that correlate with ages for evidence of regional subsidence and tsunamis during four of Cascadia's most recent plate-boundary earthquakes. Two peat–mud contacts unblanketed by sand may record small coseismic relative sea-level rises or local-to-regional rises unrelated to land-level movements during earthquake deformation cycles.

Unless substantial postseismic uplift was too rapid to be recorded, reconstruction of changes in land level from marsh core samples using diatom and foraminiferal transfer functions points to modest subsidence (0.4 ± 0.2 m)

Please cite this article as: Nelson, A.R., et al., Great-earthquake paleogeodesy and tsunamis of the past 2000 years at Alsea Bay, central Oregon coast, USA. Quaternary Science Reviews (2008), doi:10.1016/j.quascirev.2008.01.001

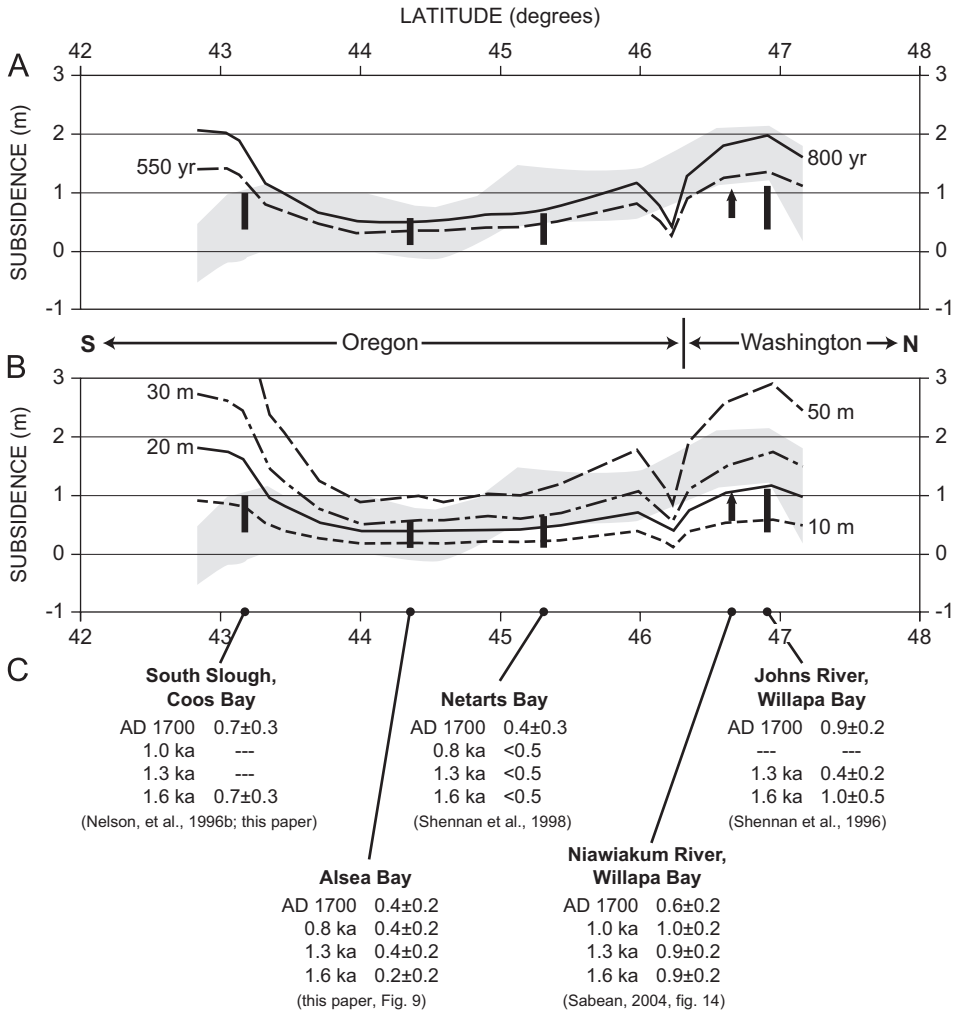

Fig. 11. Comparison of ranges of Cascadia coseismic subsidence from statistically supported microfossil studies in Oregon and Washington (vertical bars) with predictions of subsidence from elastic dislocation models (Flück et al., 1997; Wang et al., 2003) and Leonard et al.'s (2004) compilation of field subsidence data for the AD 1700 earthquake (modified from Leonard et al., 2004, Fig. 9). Gray envelopes show weighted mean $\pm 1\sigma$ of tidal wetland subsidence data compiled by Leonard et al. (2004). Bold lines show north–south variations in subsidence predicted by (A) models with complete strain release after 800 and 550-yr earthquake cycles, and (B) models of uniform slip along the length of the plate boundary of 10, 20, 30, and 50 m. (C) lists coseismic subsidence estimates for earthquakes of the indicated ages from referenced studies. Estimates for Coos Bay are derived from foraminiferal data described by Nelson et al. (1996b) using the same transfer function described in this paper. Arrows on Willapa Bay vertical bars reflect Sabean's (2004) interpretation of her estimates as minimum values. Ages for earthquakes in Oregon are from Nelson et al. (2004) and Nelson et al. (2006). Ages for Washington are from Atwater et al. (2004a).

during the four great earthquakes identified at Alsea Bay. However, interpretation is complicated by the 30–38% of potentially unreliable transfer function values from samples with poor analogs in modern diatom and foraminiferal assemblages. Reconstructions of coseismic subsidence using good-analog samples range from 0.46 ± 0.12 to 0.09 ± 0.20 m showing greater variability than implied by sample-specific function errors. Sampling at Alsea Bay is too limited and transfer functions too imprecise to argue for preseismic subsidence. These results emphasize the importance of acquiring (1) large modern data sets that sample the full range of tidal environments to improve the performance of the transfer function, and (2) fossil analyses from multiple sites in the same marsh—preferably using multiple microfossil groups—for reconstructing land-level movement during earthquake cycles.

Apparent high rates of postseismic uplift inferred from the most reliable reconstructions at Alsea Bay suggest uplift was almost as large as coseismic subsidence. The uplift may result from slip on deep parts of the plate boundary and (or) viscoelastic stress relaxation in the upper plate.

Modest coseismic subsidence is inconsistent with wide plate-boundary ruptures extending well inland of the coast. Ruptures may have been long and narrow during earthquakes near M9, as suggested for the AD 1700 earthquake, or of lower and more variable dimensions and magnitudes. Partial, coseismic strain release could explain modest subsidence during one or two of the four earthquake cycles, but probably not during all. At least for the past two millennia in central Oregon, the plate boundary ruptured largely offshore.

Please cite this article as: Nelson, A.R., et al., Great-earthquake paleogeodesy and tsunamis of the past 2000 years at Alsea Bay, central Oregon coast, USA. Quaternary Science Reviews (2008), doi:10.1016/j.quascirev.2008.01.001

Acknowledgments

This work was supported by the Earthquake Hazards Reduction Program of the US Geological Survey; diatom studies by Sawai were supported by the Geological Survey of Japan. Roger Lewis (US Geological Survey, Coastal and Marine Geology Program) collected diatom samples and did most of the leveling with the support of Eileen Hemphill-Haley (US Geological Survey, Coastal and Marine Geology Program). George McKibbin of Simpson Timber, Inc. gave permission for our work in the marshes of eastern Alsea Bay, and Robert Anthony provided advice and access to Simpson property. Rob Witter (Oregon Dept of Geology) assisted with vibrocoring, and he, Andrea Hawkes (Dept. of Earth and Environmental Science, University of Pennsylvania), and Lucinda Leonard (Earth and Ocean Sciences, University of Victoria) provided critical review of an earlier version of the paper. We appreciate reviews by Roland Gehrels and an anonymous reviewer.

Appendix A. Supplementary Materials

Supplementary data associated with this article can be found in the online version at doi:10.1016/j.quascirev.2008.01.001.

References

Allen, J.R.L., 2000. Morphodynamics of Holocene salt marshes: a review sketch from the Atlantic and southern North Sea coasts of Europe. Quaternary Science Reviews 19, 1155–1231.

Atwater, B.F., Hemphill-Haley, E., 1997. Recurrence intervals for great earthquakes of the past 3500 years at northeastern Willapa Bay, Washington. US Geological Survey Professional Paper 1576, 108pp.

Atwater, B.F., Stuiver, M., Yamaguchi, D.K., 1991. A radiocarbon test of earthquake magnitude at the Cascadia subduction zone. Nature 353, 156–158.

Atwater, B.F., Nelson, A.R., Clague, J.J., Carver, G.A., Bobrowsky, P.T., Bourgeois, J., Darienzo, M.E., Grant, W.C., Hemphill-Haley, E., Kelsey, H.M., Jacoby, C.G., Nishenko, S.P., Palmer, S., Peterson, C.D., Reinhart, M.A., Yamaguchi, D.K., 1995. Summary of coastal geologic evidence for past great earthquakes at the Cascadia subduction zone. Earthquake Spectra 11, 1–18.

Atwater, B.F., Tuttle, M.P., Schweig, E.S., Rubin, C.M., Yamaguchi, D.K., Hemphill-Haley, E., 2004a. Earthquake recurrence inferred from paleoseismology. In: Gillespie, A.R., Porter, S.C., Atwater, B.F. (Eds.), The Quaternary Period in the United States. Developments in Quaternary science. Elsevier, New York, pp. 331–350.

Atwater, B.F., Furukawa, R., Hemphill-Haley, E., Ikeda, Y., Kashima, K., Kawase, K., Kelsey, H.M., Moore, A.L., Nanayama, F., Nishimura, Y., Odagiri, S., Ota, Y., Park, S.-C., Satake, K., Sawai, Y., Shimokawa, K., 2004b. Seventeenth-century uplift in eastern Hokkaido, Japan. The Holocene 14, 487–501.

Atwater, B.F., Musumi-Rokkaku, S., Satake, K., Tsuji, Y., Ueda, K., Yamaguchi, D.K., 2005. The orphan tsunami of 1700-Japanese clues to a parent earthquake in North America. US Geological Survey Professional Paper 1707, 133pp (published jointly by University of Washington Press, Seattle, Washington).

Benson, B.E., Grimm, K.A., Clague, J.J., 1997. Tsunami deposits beneath tidal marshes on northwestern Vancouver Island, British Columbia. Quaternary Research 48, 192–204.

Birks, H.J.B., 1995. Quantitative palaeoenvironmental reconstructions. In: Maddy, D., Brew, J. (Eds.), Statistical Modeling of Quaternary Science Data. Technical Guide No. 5. Quaternary Research Association, Cambridge, UK, pp. 161–236.

Bourgeois, J., Pinegina, T.K., Ponomareva, V., Zaretskala, N., 2006. Holocene tsunamis in the southwestern Bering Sea, Russian Far East, and their tectonic implications. Bulletin of the Geological Society of America 118, 449–463.

Briggs, R.W., Sieh, K., Meltzner, A.J., Natawidjaja, D., Galetzka, J., Suwrgadi, B., Hsu, Y., Simons, M., Hananto, N., Suprihanto, I., Prayudi, D., Avouac, J.-P., Prawirodirdjo, L., Bock, Y., 2006. Deformation and slip along the Sunda Megathrust in the great 2005 Nias-Simeulue earthquake. Science 311, 1897–1901.

Bronk Ramsey, C., 1995. Radiocarbon calibration and analysis of stratigraphy, the OxCal program. Radiocarbon 37, 425–430.

Bronk Ramsey, C., 2001. Development of the radiocarbon program OxCal. Radiocarbon 43, 355–363.

Chlieh, M., Avouac, J.-P., Hjorleifsdottir, V., Song, T.R.A., Ji, C., Sieh, K., Sladen, A., Hebert, H., Prawirodirdjo, L., Bock, Y., Galetzka, J., 2007. Coseismic slip and afterslip of the great Mw9.15 Sumatra-Andaman earthquake of 2004. Bulletin of Seismological Society of America 97, S152–S173.

Cisternas, V.M, Atwater, B.F., Torrejón, F., Sawai, Y., Machuca, G., Lagos, M., Eipert, A., Youlton, C., Salgado, I., Kamataki, T., Shishikura, M., Rajendran, C.P., Malik, J.K., Rizal, Y., Husni, M., 2005. Predecessors to the giant 1960 Chile earthquake. Nature 437, 404–407.

Clague, J.J., 1997. Evidence for large earthquakes at the Cascadia subduction zone. Reviews of Geophysics 35, 439–460.

Clague, J.J., Atwater, B.F., Wang, K., Wang, Y., Wong, I., (Compilers) 2000a. Penrose Conference 2000, Great Cascadia Earthquake Tricentennial, Program Summary and Abstracts. Geological Society of America Penrose Conference on Great Cascadia Earthquake Tricentennial, Seaside, Oregon, 2–8 June 2001, Oregon Department of Geology and Mineral Industries Special Paper 33, 156pp.

Clague, J.J., Bobrowsky, P.T., Hutchinson, I., 2000b. A review of geological records of large tsunamis at Vancouver Island, British Columbia, and implications for hazard. Quaternary Science Reviews 19, 849–863.

Crawford, R.M., 1979. Taxonomy and frustular structure of the marine centric diatom *Paralia sulcata*. Journal of Phycology 15, 200–210.

Darienzo, M.E., Peterson, C.D., 1995. Magnitude and frequency of subduction-zone earthquakes along the northern Oregon coast in the past 3000 years. Oregon Geology 57, 3–12.

Darienzo, M.E., Peterson, C.D., Clough, C., 1994. Stratigraphic evidence for great subduction-zone earthquakes at four estuaries in northern Oregon. USA Journal of Coastal Research 10, 850–876.

Denys, L., de Wolf, H., 1999. Diatoms as indicators of coastal paleoenvironments and relative sea-level change. In: Stoermer, E.F., Smol, J.P. (Eds.), The Diatoms: Applications for the Environmental and Earth Sciences. Cambridge University Press, Cambridge, UK, pp. 277–297.

de Rijk, S., Troelstra, S.R., 1997. Salt marsh foraminifera from the Great Marshes, Massachusetts: environmental controls. Palaeogeography, Palaeoclimatology, Palaeoecology 130, 81–112.

Edwards, B.P., Horton, B.P., 2000. Reconstructing relative sea-level change using UK salt-marsh foraminifera. Marine Geology 169, 41–56.

Elder, K.L., McNichol, A.P., Gagnon, A.R., 1998. Evaluating reproducibility of seawater, inorganic and organic carbon ^{14}C results at the National Ocean Sciences AMS Facility (NOSAMS). Radiocarbon 40, 223–230.

Flück, P., Hyndman, R.D., Wang, K., 1997. Three-dimensional dislocation model for great earthquakes of the Cascadia subduction zone. Journal of Geophysical Research 102, 20539–20550.

Frankel, A.D., Petersen, M.D., Mueller, C.S., Haller, K.M., Wheeler, R.L., Leyendecker, E.V., Wesson, R.L., Harmsen, S.C., Cramer, C.H., Perkins, D.M., Rukstales, K.S., 2002. Documentation for the 2002

update of the national seismic hazard maps. US Geological Survey Open-File Report 02-420, 33pp. 〈http://geohazards.cr.usgs.gov/eq/of02-420/OFR02-420.pdf〉.

Gehrels, W.R., 2000. Using foraminiferal transfer functions to produce high-resolution sea-level records from salt-marsh deposits, Maine, USA. The Holocene 10, 367–376.

Gehrels, W.R., Roe, H.M., Charman, D.J., 2001. Foraminifera, testate amoebae and diatoms as sea-level indicators in UK salt marshes: a quantitative multiproxy approach. Journal of Quaternary Science 16, 201–220.

Goldfinger, C., Nelson, C.H., Johnson, J.F., 2003. Holocene earthquake records from the Cascadia subduction zone and northern San Andreas fault based on precise dating of offshore turbidites. Annual Review of Earth and Planetary Sciences 31, 555–577.

Goldstein, S.T., Watkins, G.T., 1999. Taphonomy of salt marsh foraminifera: an example from coastal Georgia. Palaeogeography, Palaeoclimatology, Palaeoecology 149, 103–114.

Goodwin, C.R., Emmett, E.W., Glenne, B., 1970. Tidal Study of Three Oregon Estuaries. Bulletin No. 45. Engineering Experiment Station, Oregon State University, Corvallis Oregon, 32pp.

Guilbault, J.-P., Clague, J.J., Lapointe, M., 1995. Amount of subsidence during a late Holocene earthquake—evidence from fossil tidal marsh foraminifera at Vancouver Island, west coast of Canada. Palaeogeography, Palaeoclimatology, Palaeoecology 118, 49–71.

Guilbault, J.-P., Clague, J.J., Lapointe, M., 1996. Foraminiferal evidence for the amount of coseismic subsidence during a late Holocene earthquake on Vancouver Island, west coast of Canada. Quaternary Science Reviews 15, 913–937.

Hamilton, S.L., Shennan, I., 2005a. Late Holocene land and sea-level changes and the earthquake deformation cycle around the upper Cook Inlet, Alaska. Quaternary Science Reviews 24, 1479–1498.

Hamilton, S.L., Shennan, I., 2005b. Late Holocene great earthquakes and relative sea-level change at Kenai, southern Alaska. Journal of Quaternary Science 20, 95–111.

Hamilton, S.L., Shennan, I., Combellick, R., Mulholland, J., Noble, C., 2005. Evidence for two great earthquakes at Anchorage, Alaska, and implications for multiple great earthquakes through the Holocene. Quaternary Science Reviews 24, 2050–2068.

Hammer, O., Harper, D.A.T., Ryan, P.D., 2006. PAST–PAlaeontological STatistics, version 1.56. 〈http//folk.uio.no/ohammer/past/〉.

Hawkes, A.D., Scott, D.B., Lipps, J.H., Combellick, R., 2005. Evidence for possible precursor events of megathrust earthquakes on the west coast of North America. Geological Society of America Bulletin 117, 996–1008.

Hemphill-Haley, E., 1995. Diatom evidence for earthquake-induced subsidence and tsunami 300 yr ago in southern coastal Washington. Geological Society of America Bulletin 107, 367–378.

Hemphill-Haley, E., 1996. Diatoms as an aid in identifying late-Holocene tsunami deposits. The Holocene 6, 439–448.

Hippensteel, S.P., Martin, R.E., Nikitina, D., Pizzuto, J.E., 2002. Interannual variation of marsh foraminiferal assemblages (Bombay Hook Wildlife Refuge, Symrna, DE): do foraminiferal assemblages have a memory? Journal of Foraminiferal Research 32, 97–109.

Horton, B.P., 1999. The contemporary distribution of intertidal foraminifera of Cowpen Marsh, Tees Estuary, UK: implications for studies of Holocene sea-level changes. Palaeogeography, Palaeoclimatology, Palaeoecology 149, 127–149.

Horton, B.P., Edwards, B.P., 2003. Seasonal distributions of foraminifera and their implications for sea-level studies, Cowpen Marsh, UK SEPM Society for Sedimentary Geology Special Publication No. 75, pp. 21–30.

Horton, B.P., Edwards, R.J., 2005. The application of local and regional transfer functions to the reconstruction of Holocene sea levels, north Norfolk, England. The Holocene 15, 216–228.

Horton, B.P., Edwards, B.P., 2006. Quantifying Holocene sea-level change using intertidal foraminifera: lessons from the British Isles. Cushman Foundation for Foraminiferal Research, Special Publication No. 40, 97pp.

Horton, B.P., Edwards, B.P., Lloyd, J.M., 1999a. A foraminiferal-based transfer function implications for sea-level studies. Journal of Foraminiferal Research 29, 117–129.

Horton, B.P., Edwards, B.P., Lloyd, J.M., 1999b. UK intertidal foraminiferal distributions: implications for sea-level studies. Marine Micropaleontology 36, 205–223.

Hu, Y., Wang, K., He, J., Klotz, J., Khazaradze, G., 2004. Three-dimensional viscoelastic finite element model for postseismic deformation of the great 1960 Chile earthquake. Journal of Geophysical Research Solid Earth 109 (B12), doi:10.1029/2004JB003163.

Hughes, J.F., Mathewes, R.W., Clague, J.J., 2002a. Use of pollen and vascular plants to estimate coseismic subsidence at a tidal marsh near Tofino, British Columbia. Palaeogeography, Palaeoclimatology, Palaeoecology 185, 145–161.

Hughes, J.F., Mathewes, R.W., Clague, J.J., Guilbault, J.-P., Hutchinson, I., 2002b. Rapid crustal rebound followed the 1700 Cascadia earthquake at Tofino, British Columbia [abstract]. Seismological Research Letters 73, 241.

Hyndman, R.D., Wang, K., 1995. The rupture zone of Cascadia great earthquakes from current deformation and the thermal regime. Journal of Geophysical Research 100, 22133–22154.

Hyndman, R.D., Leonard, L.J., Currie, C.A., 2005. Test of models for the Cascadia great earthquake rupture area using coastal subsidence estimates for the 1700 earthquake. Final Report, US Geological Survey NEHRP External Grant Award 04HQGR0088, 11pp.

Jennings, A.E., Nelson, A.R., 1992. Foraminiferal assemblage zones in Oregon tidal marshes—relation to marsh floral zones and sea level. Journal of Foraminiferal Research 22, 13–29.

Jennings, A.E., Nelson, A.R., Scott, D.B., Aravena, J.-C., 1995. Marsh foraminiferal assemblages in the Valdivia estuary, south-central Chile, relative to vascular plants and sea level. Journal of Coastal Research 11, 107–123.

Juggins, S., 2003. C2 User Guide: Software for Ecological and Palaeoecological Data Analysis and Visualisation. University of Newcastle, Newcastle upon Tyne, UK, 69pp.

Kelsey, H.M., Witter, R.C., Hemphill-Haley, E., 2002. Plate-boundary earthquakes and tsunamis of the past 5500 years, Sixes River estuary, southern Oregon. Geological Society of America Bulletin 114, 298–314.

Kelsey, H.M., Nelson, A.R., Hemphill-Haley, E., Witter, R., 2005. Tsunami history of an Oregon coastal lake reveals a 4600 yr record of great earthquakes on the Cascadia subduction zone. Geological Society of America Bulletin 117, 1009–1032.

Leonard, L.J., Hyndman, R.D., Mazzotti, S., 2004. Coseismic subsidence in the 1700 great Cascadia earthquake coastal estimates versus elastic dislocation models. Geological Society of America Bulletin 116, 655–670.

Long, A.J., Shennan, I., 1994. Sea-level changes in Washington and Oregon and the "earthquake deformation cycle". Journal of Coastal Research 10, 825–838.

Long, A.J., Shennan, I., 1998. Models of rapid relative sea-level change in Washington and Oregon, USA. The Holocene 8, 129–142.

Long, A.J., Innes, J.B., Shennan, I., Tooley, M.J., 1999. Coastal stratigraphy a case study from Johns River, Washington, USA. In: Jones, A.P., Tucker, M.E., Hola, J.K. (Eds.), The Description and Analysis of Quaternary Stratigraphic Field Sections. Technical Guide 7. Quaternary Research Association, London, UK, pp. 267–286.

Martin, R.E., Hippensteel, S.P., Nikitina, D., Pizzuto, J.E., 2003. Taphonomy and artificial time-averaging of marsh foraminiferal assemblages (Bombay Hook National Wildlife Refuge, Smyrna, Delaware, USA): implications for rates and magnitudes of late Holocene sea-level change. In: Micropaleontologic Proxies for Sea-Level Change and Stratigraphic Discontinuities. Society for Sedimentary Geology Special Publication No. 75, pp. 31–49.

Morton, R.A., Gelfenbaum, G., Jaffe, B.E., 2007. Physical criteria for distinguishing sandy tsunami and storm deposits using modern examples. Sedimentary Geology 200, 184–207.

Please cite this article as: Nelson, A.R., et al., Great-earthquake paleogeodesy and tsunamis of the past 2000 years at Alsea Bay, central Oregon coast, USA. Quaternary Science Reviews (2008), doi:10.1016/j.quascirev.2008.01.001

Murray, J.W., 2000. The enigma of the continued use of total assemblages in ecological studies of benthic foraminifera. Journal of Foraminiferal Research 30, 244–245.

Nanayama, F., Shigeno, K., Satake, K., Shimokawa, K., Koitabashi, S., Miyasaka, S., Ishii, M., 2000. Sedimentary differences between the 1993 Hokkaido-naisei-oki tsunami and the 1959 Miyakojima typhoon at Taisei, southwestern Hokkaido, northern Japan. Sedimentary Geology 155, 129–145.

Natawidjaja, D.H., Sieh, K., Ward, S.N., Cheng, H., Edwards, R.L., Galetka, J., Suwargadi, W., 2004. Paleogeodetic records of seismic and aseismic subduction from central Sumatran microatolls, Indonesia. Journal of Geophysical Research Solid Earth 109, B04306, doi:10.1029/2003.

National Ocean Service, 1987. Tide Tables, 1988—West Coast of North and South America. US Department of Commerce, National Oceanic and Atmospheric Administration, Washington, DC.

Nelson, A.R., 1992. Discordant ^{14}C ages from buried tidal-marsh soils in the Cascadia subduction zone, southern Oregon coast. Quaternary Research 38, 74–90.

Nelson, A.R., Kashima, K., 1993. Diatom zonation in southern Oregon tidal marshes relative to vascular plants, foraminifera, and sea level. Journal of Coastal Research 9, 673–697.

Nelson, A.R., Personius, S.F., 1996. The potential for great earthquakes in Oregon and Washington—an overview of recent coastal geologic studies and their bearing on segmentation of Holocene ruptures, central Cascadia subduction zone. In: Rogers, A.M., Walsh, T.J., Kockelman, W.J., Priest, G.R. (Eds.), Assessing Earthquake Hazards and Reducing Risk in the Pacific Northwest. US Geological Survey Professional Paper 1560, vol. 1, pp. 91–114.

Nelson, A.R., Atwater, B.F., Bobrowsky, P.T., Bradley, L.-A., Clague, J.J., Carver, G.A., Darienzo, M.E., Grant, W.C., Krueger, H.W., Sparks, R., Stafford Jr., T.W., Stuiver, M., 1995. Radiocarbon evidence for extensive plate-boundary rupture about 300 years ago at the Cascadia subduction zone. Nature 378, 371–374.

Nelson, A.R., Shennan, I., Long, A.J., 1996a. Identifying coseismic subsidence in tidal-wetland stratigraphic sequences at the Cascadia subduction zone of western North America. Journal of Geophysical Research 101 (B3), 6115–6135.

Nelson, A.R., Jennings, A.E., Kashima, K., 1996b. An earthquake history derived from stratigraphic and microfossil evidence of relative sea-level change at Coos Bay, southern coastal Oregon. Geological Society of America Bulletin 108, 141–154.

Nelson, A.R., Ota, Y., Umitsu, M., Kashima, K., Matshushima, Y., 1998. Seismic or hydrodynamic control of rapid late-Holocene sea-level rise in southern coastal Oregon, USA? The Holocene 8, 287–299.

Nelson, A.R., Asquith, A.C., Grant, W.C., 2004. Great earthquakes and tsunamis of the past 2000 years at the Salmon River estuary, central Oregon coast, USA. Bulletin of Seismological Society of America 94, 1276–1292.

Nelson, A.R., Kelsey, H.M., Hemphill-Haley, E., Witter, R.C., 2006. Great earthquakes of variable magnitude at the Cascadia subduction zone. Quaternary Research 65, 354–365.

Ozarko, D.L., Patterson, R.T., Williams, H.F.L., 1997. Marsh foraminifer from Nanaimo, British Columbia, Canada: implications of infaunal habitat and taphonomic biasing. Journal of Foraminiferal Research 27, 51–68.

Patterson, R.T., Guilbault, J.-P., Clague, J.J., 1999. Taphonomy of tidal marsh foraminifera implications of surface sample thickness for high-resolution sea-level studies. Palaeogeography, Palaeoclimatology, Palaeoecology 149, 199–211.

Patterson, R.T., Gehrels, W.R., Belknap, D.F., Dalby, A.P., 2004. The distribution of salt marsh foraminifera at Little Dipper Harbour, New Brunswick, Canada: implications for development of widely applicable transfer functions in sea-level research. Quaternary International 120, 185–194.

Patterson, R.T., Dalby, A.P., Roe, H.M., Guilbault, J.-P., Hutchinson, I., Clague, J.J., 2005. Relative utility of foraminifera, diatoms, and macrophytes as high resolution indicators of paleo-sea level in coastal British Columbia, Canada. Quaternary Science Reviews 24, 2002–2014.

Peterson, C.D., Darienzo, M.E., 1996. Discrimination of climatic, oceanic, and tectonic mechanisms of cyclic marsh burial, Alsea Bay, Oregon. In: Rogers, A.M., Walsh, T.J., Kockelman, W.J., Priest, G.R. (Eds.), Assessing Earthquake Hazards and Reducing Risk in the Pacific Northwest. US Geological Survey Professional Paper 1560, vol. 1, pp. 115–146.

Peterson, C.D., Doyle, D.L., Barnett, E.T., 2000. Coastal flooding and beach retreat from coseismic subsidence in the central Cascadia margin, USA. Environmental and Engineering Geoscience 6, 255–269.

Priest, G.R., Allan, J.C., 2003. Tsunami hazard map of the Alsea Bay-Waldport area, Lincoln County, Oregon. Oregon Department of Geology and Mineral Industries, Interpretive Map Series, IMS-23.

Reimer, P.J., Baillie, M.G.L., Bard, E., Bayliss, A., Beck, J.W., Bertrand, C.J.H., Blackwell, P.G., Buck, C.E., Burr, G.S., Cutler, K.B., Damon, P.E., Edwards, R.L., Fairbanks, R.G., Friedrich, M., Guilderson, T.P., Hogg, A.G., Hughen, K.A., Kromer, B., McCormac, G., Manning, S., Bronk Ramsey, C., Reimer, R.W., Remmele, S., Southon, J.R., Stuiver, M., Talamo, S., Taylor, F.W., van der Plicht, J., Weyhenmeyer, C.E., 2004. IntCal04 terrestrial radiocarbon age calibration, 0–26 cal kyr BP. Radiocarbon 46, 1029–1058.

Sabean, J.A.R., 2004. Applications of foraminifera to detecting land level change associated with great earthquakes along the west coast of North America. M.S. Thesis, Department of Earth Sciences, Simon Fraser University, Burnaby, Bristish Columbia, 90pp.

Satake, K., Atwater, B.F., 2007. Long-term perspectives on giant earthquakes and tsunamis at subduction zones. Annual Review of Earth and Planetary Sciences 35, 349–374.

Satake, K., Wang, K., Atwater, B.F., 2003. Fault slip and seismic moment of the 1700 Cascadia earthquake inferred from Japanese tsunami descriptions. Journal of Geophysical Research Solid Earth 108 (B11), 2535, doi:10.1029/2003JB002521.

Sawai, Y., 2001. Distribution of living and dead diatoms in tidal wetlands of northern Japan: relations to taphonomy. Palaeogeography, Palaeoclimatology, Palaeoecology 173, 125–141.

Sawai, Y., 2002. Evidence for 17th-century tsunamis generated on the Kuril-Kamchatka subduction zone, Lake Tokotan, Hokkaido, Japan. Journal of Asian Earth Sciences 20, 903–911.

Sawai, Y., Nagumo, T., 2003. Diatoms from Alsea Bay, Oregon, USA. Diatom, The Japanese Society of Diatomology 19, 33–46.

Sawai, Y., Horton, B.P., Nagumo, T., 2004a. The development of a diatom-based transfer function along the Pacific coast of eastern Hokkadio, northern Japan-an aid in paleoseismic studies of the Kurile subduction zone. Quaternary Science Reviews 23, 2467–2483.

Sawai, Y., Satake, K., Takanobu, K., Nasu, H., Shishikura, M., Atwater, B.F., Horton, B.P., Kelsey, H.M., Nagumo, T., Yamaguchi, M., 2004b. Transient uplift after a 17th-century earthquake along the Kuril subduction zone. Science 306, 1918–1920.

Sawai, Y., Nagumo, T., Toyoda, K., 2005. Three extant species of *Paralia* Bacillariophyceae along the coast of Japan. Phycologia 445, 517–529.

Schlichting, R.B., Peterson, C.D., 2006. Mapped overland distance of paleotsunami high-velocity inundation in back-barrier wetlands of the central Cascadia margin, USA. Journal of Geology 114, 577–592.

Schmidt, D., Burgette, R., Weldon, R., 2007. The distribution of interseismic locking on the central Cascadia subduction zone inferred from coastal uplift rates in Oregon. EOS, Transactions AGU 88(52), Fall Meeting Supplement, Abstract T52A-04.

Scott, D.K., Leckie, R.M., 1990. Foraminiferal zonation of Great Sippwissett Salt Marsh, Falmouth, Massachusetts. Journal of Foraminiferal Research 20, 248–266.

Shennan, I., Hamilton, S.L., 2006. Coseismic and pre-seismic subsidence associated with great earthquakes in Alaska. Quaternary Science Reviews 25, 1–8.

Shennan, I., Horton, B.P., 2002. Holocene land- and sea-level changes in Great Britain. Journal of Quaternary Science 17, 511–526.

Shennan, I., Long, A.J., Rutherford, M.M., Green, F.M., Innes, J.B., Lloyd, J.M., Zong, Y., Walker, K.J., 1996. Tidal marsh stratigraphy, sea-level change and large earthquakes, I: a 5000 year record in Washington, USA. Quaternary Science Reviews 15, 1023–1059.

Please cite this article as: Nelson, A.R., et al., Great-earthquake paleogeodesy and tsunamis of the past 2000 years at Alsea Bay, central Oregon coast, USA. Quaternary Science Reviews (2008), doi:10.1016/j.quascirev.2008.01.001

Shennan, I., Long, A.J., Rutherford, M.M., Innes, J.B., Green, F.M., Kirby, J.R., Walker, K.J., 1998. Tidal marsh stratigraphy, sea-level change and large earthquakes, II: submergence events during the last 3500 years at Netarts Bay, Oregon, USA. Quaternary Science Reviews 17, 365–393.

Shennan, I.A., Scott, D.B., Rutherford, M., Zong, Y., 1999. Microfossil analysis of sediments representing the 1964 earthquake, exposed at Girdwood Flats, Alaska, USA. Quaternary International 60, 55–73.

Sherrod, B.L., 2001. Evidence for earthquake-induced subsidence about 1100 yr ago in coastal marshes of southern Puget Sound, Washington. Geological Society of America 113, 1299–1311.

Soeda, Y., Nanayama, F., Shigeno, K., Furukawa, R., Kumasaki, N., Ishii, M., 2004. Large prehistorical tsunami traces at the historical site of Kokutaiji Temple and the Shiomigawa lowland, eastern Hokkaido: significance of sedimentological and diatom analyses for identification of past tsunami deposits. Memoirs Geological Society of Japan (58), 63–75.

Taylor, R.E., Stuiver, M., Reimer, P.J., 1996. Development and extension of the calibration of the radiocarbon time scale archaeological applications. Quaternary Science Reviews 15, 655–668.

Troels-Smith, J., 1955. Characterization of unconsolidated sediments. Geological Survey of Denmark, Series IV 3, No. 10, 72pp.

Tuttle, M.P., Ruffman, A., Anderson, T., Jeter, H., 2004. Distinguishing tsunami from storm deposits in eastern North America: the 1929 Grand Banks tsunami versus the 1991 Halloween storm. Seismological Research Letters 75, 117–131.

Uchida, N., Hasegawa, A., Matsuzawa, T., Igarashi, T., 2004. Pre- and post-seismic slow slip on the plate boundary off Sanriku, NE Japan associated with three interplate earthquakes as estimated from small repeating earthquake data. Tectonophysics 385, 1–15.

Wang, K., 2007. Elastic and viscoelastic models of crustal deformation in subduction earthquake cycles. In: Dixon, T., Moore, J.C. (Eds.), The Seismogenic Zone of Subduction Thrust Faults. Columbia University Press, New York, pp. 540–575.

Wang, K., Wells, R.E., Mazzotti, R.D., Hyndman, R.D., Sagiya, T., 2003. A revised dislocation model of interseismic deformation of the Cascadia subduction zone. Journal of Geophysical Research 108, doi:10.1029/2001JB001227.

Wells, R.E., Blakely, R.J., Sugiyama, Y., Scholl, D.W., Dinterman, P.A., 2003. Basin-centered asperities in great subduction zone earthquakes: a link between slip, subsidence, and subduction erosion? Journal of Geophysical Research 108 (B10), 2507, doi:10.1029/2002JB002072.

Whiting, M.C., McIntire, C.D., 1985. An investigation of distributional patterns in the diatom flora of Netarts Bay, Oregon, by correspondence analysis. Journal of Phycology 21, 655–661.

Williams, H.F.L., Hutchinson, I., Nelson, A.R., 2005. Multiple sources for late Holocene tsunamis at Discovery Bay, Washington State, USA. The Holocene 15, 60–73.

Witter, R.C., Kelsey, H.M., Hemphill-Haley, E., 2001. Pacific storms, El Nino and tsunamis: competing mechanisms for sand deposition in a coastal marsh, Euchre Creek, Oregon. Journal of Coastal Research 17, 563–583.

Witter, R.C., Kelsey, H.M., Hemphill-Haley, E., 2003. Great Cascadia earthquakes and tsunamis of the past 6700 years, Coquille River estuary, southern coastal Oregon. Geological Society of America Bulletin 115, 1289–1306.

Yoshioka, S., Wang, K., Mazzotti, S., 2005. Interseismic locking of the plate interface in the northern Cascadia subduction zone, inferred from inversion of GPS data. Earth and Planetary Science Letters 231, 239–247.

Zong, Y., Horton, B.P., 1999. Diatom-based tidal-level transfer functions as an aid in reconstructing Quaternary history of sea-level movements in the UK. Journal of Quaternary Science 14, 153–167.

Zong, Y., Shennan, I., Combellick, R.A., Hamilton, S.L., Rutherford, M.M., 2003. Microfossil evidence for land movements associated with the AD 1964 Alaska earthquake. The Holocene 13, 7–20.

Please cite this article as: Nelson, A.R., et al., Great-earthquake paleogeodesy and tsunamis of the past 2000 years at Alsea Bay, central Oregon coast, USA. Quaternary Science Reviews (2008), doi:10.1016/j.quascirev.2008.01.001